CHAPTER 5 RESULTS AND DISCUSSION

5.1 Introduction

This Chapter presents and explains the results obtained from the present FEA using the adopted modeling technique described in Chapter 3. More specifically, a variety of bridge decks are modeled based on the variation of general physical parameters mentioned in Chapter 4. These range from the bridges with N_G of 3 to 7 and S of 1.52 (5 ft) to 3.66 m (12 ft), which lead to W of 4.88 (16 ft) to 11 m (36 ft). In view of the conservative aspect, each model has the same girder series of W33 wide-flange sections I-beams and the same slab thickness of 200 mm (8 in). Next, the maximum M_{LL}^{-} and M_{LL}^{+} are therefore determined for each ***BC***, ***y*** and N_L based on trial and error analysis of truck position on bridge deck as mentioned in Chapter 4 (section 4.3 and 4.4). This Chapter begins with demonstration of the effects of considered parameters on M_{LL}^{-} and M_{LL}^{+}. After that, the comparison between results obtained in the literature (Westergaard, 1930; BS 5400, 2005; Cao, and Shing, 1999; AASHTO, 2002; AASHTO, 2004; CAN/CSA-S6-06, 2006) and the ones obtained using present FEA is made. Finally, the FEA-based formulas are proposed to directly compute M_{LL}^{-} and M_{LL}^{+} for the practical application. Note that these resulting moments are presented in term of moment per unit length of slab (kN-m/m).

At this time, the variations of a dimensionless ratio of M_{LL}^{-}/P and M_{LL}^{+}/P (P stands for a HS20-44 truck wheel load of 71.172 kN or 16 kips) obtained from the present FEA are expressed with respect to the general physical, loading location and traffic characteristic parameters. It should be noted that the maximum values of these moments are selected among those obtained from several FEA models with variation of ***BC*** and positions of truck wheels on the bridge deck. The general trends of M_{LL}^{-}/P and M_{LL}^{+}/P (excluding self weight) regarding the effect of those considered parameters are subsequently described in section 5.2 and 5.3, respectively.

5.2 Effects of Present Parameters on M_{LL}^{-}

The effects of influential parameters on $M_{LL}^{-}/\boldsymbol{P}$ are discussed in this section. The numerical results of $M_{LL}^{-}/\boldsymbol{P}$ with respect to the considered parameters can be pointed out as follows:

5.2.1 Effect of Spacing of Girder

To capture the influence of girder spacing S on M^-_{LL}/P, a dimensionless ratio of S/S_{MIN} will be adopted herein for a useful presentation. Figure 5.1 shows the typical effects of S/S_{MIN} on M^-_{LL}/P for each considered N_L at three different locations of y. The numerical results indicate that S/S_{MIN} has significant influence on M^-_{LL}/P: as S/S_{MIN} becomes larger, M^-_{LL}/P increases in general, especially at the support and quarter span regions. However, at the mid span the effect of S seems to be smaller as proved by the lesser steep curves in Figure 5.1 (c). Moreover, the deck hogging due to a specific loading pattern (N_L = 2) trends to induce lower M^-_{LL}/P at the quarter span as demonstrated in Figure 5.1 (b). Nevertheless, at the mid span, the effect of deck hogging can result in the raising of M^-_{LL}/P as shown in Figure 5.1 (c).

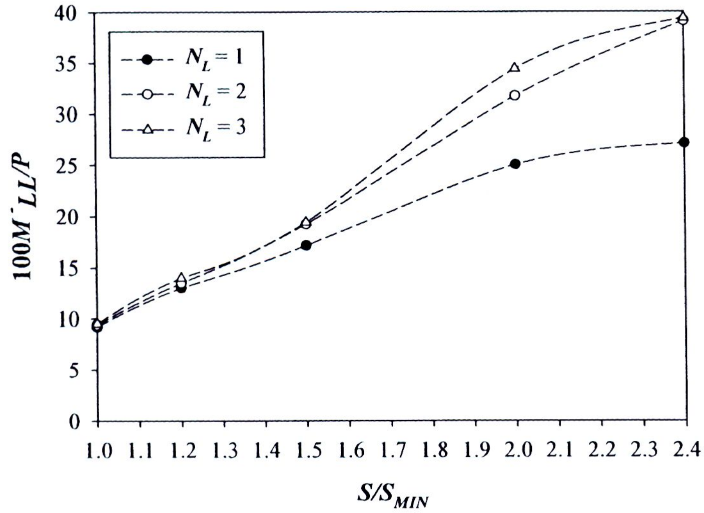

(a) At support

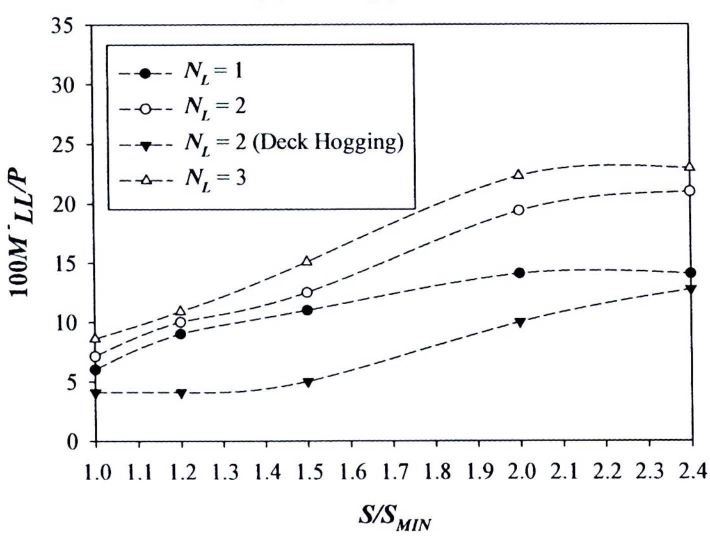

(b) At quarter span

Figure 5.1 Variation of M^-_{LL}/P with respect to S/S_{MIN}: (a) At support; (b) At quarter span; (c) At mid span

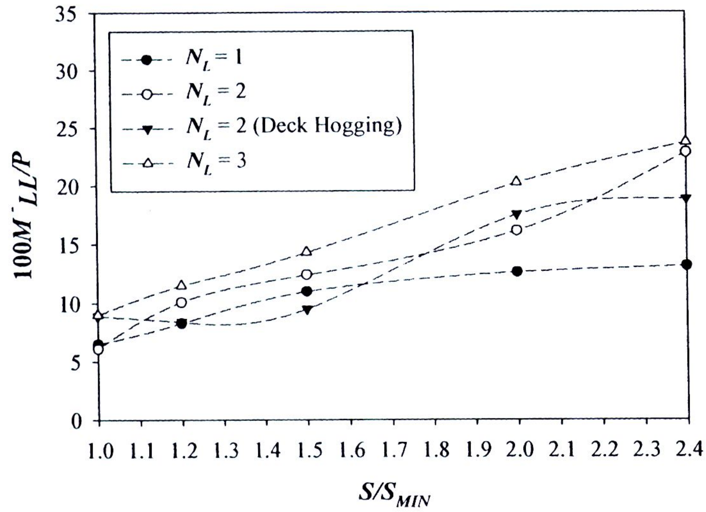

(c) At mid span

Figure 5.1 (Con't) Variation of M^-_{LL}/P with respect to S/S_{MIN}: (a) At support; (b) At quarter span; (c) At mid span

5.2.2 Effect of Loading Location

Figure 5.2 shows the effect of loading location along bridge span denoted by the parameter *y* on M^-_{LL}/P for each N_L. It has been observed that *y* has a significant influence on M^-_{LL}/P for large S/S_{MIN} ($S/S_{MIN} \geq 1.5$). Nevertheless, the effect of *y* appears to be lesser when the value of S/S_{MIN} is smaller than 1.2. It has been also found out that the effect of *y* is largest as it induces M^-_{LL}/P quite higher at the support and rapidly reduces at the quarter and mid span.

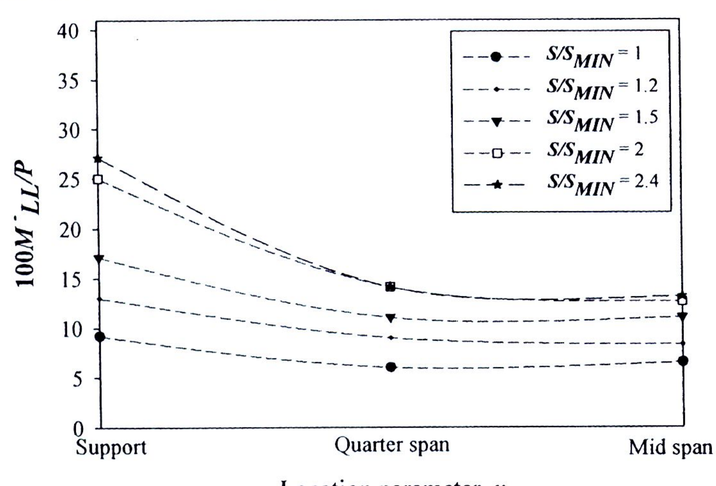

(a) $N_L = 1$

Figure 5.2 Variation of M^-_{LL}/P with respect to *y*: (a) $N_L = 1$; (b) $N_L = 2$; (c) $N_L = 3$

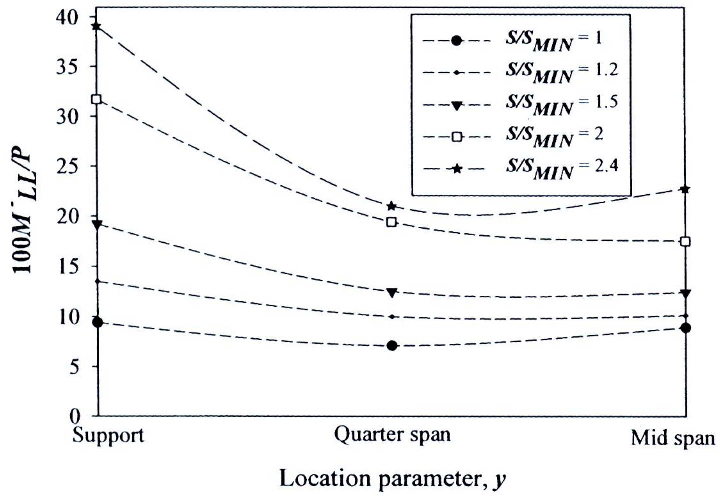

(b) $N_L = 2$

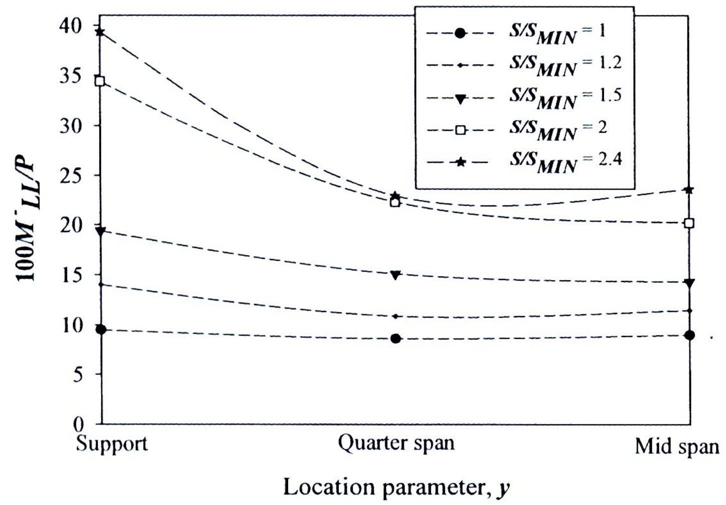

(c) $N_L = 3$

Figure 5.2 (Con't) Variation of M^-_{LL}/P with respect to y: (a) $N_L = 1$; (b) $N_L = 2$; (c) $N_L = 3$

5.2.3 Effect of Traffic Characteristic

Due to its transient loading, the truck can move anywhere within the traffic lane. This leads to the difficulty in determination of truck position that produces the critical effect on M^-_{LL}. To be able to fulfill this complexity, the effect of traffic characteristic on M^-_{LL}/P can be alternatively expressed through the consideration of parameter N_L. In particular, the critical pattern of truck loading can be determined according to the trial and error analysis for each different y as mentioned in Chapter 4. For each N_L, the maximum M^-_{LL}/P can be then obtained and plotted against the corresponding N_L. It has been observed from Figure 5.3 that M^-_{LL}/P tends to grow with the increase of N_L. As the number of N_L increases, the gradient of M^-_{LL}/P gradually increases for $S/S_{MIN} \leq 1.5$. However, the effect of N_L on M^-_{LL}/P is obviously mounting when $S/S_{MIN} \geq 2$.

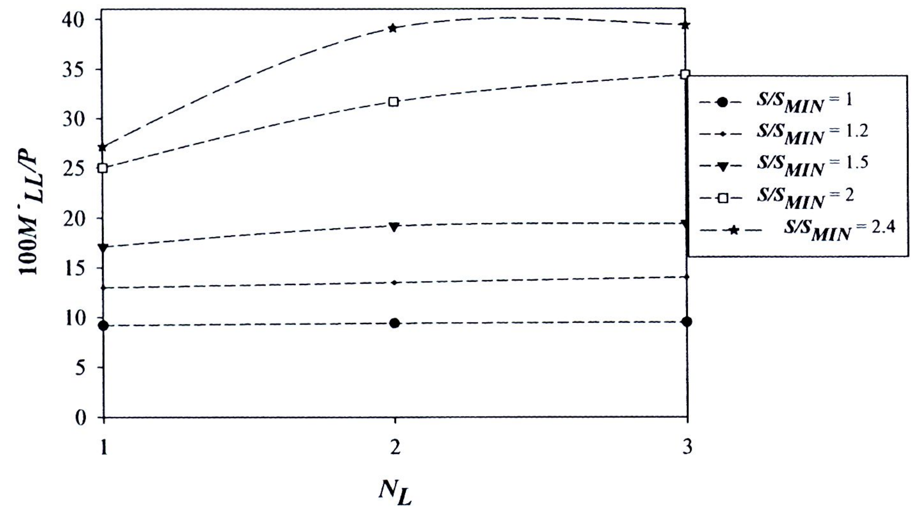

(a) At support

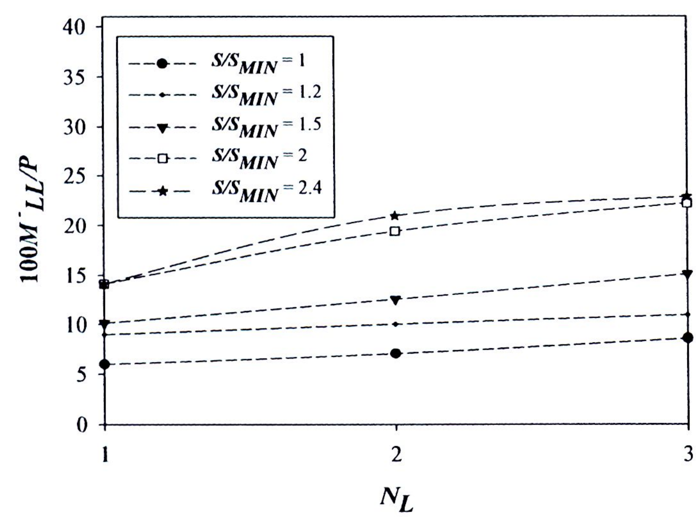

(b) At quarter span

Figure 5.3 Variation of M^-_{LL}/P with respect to N_L:
(a) At support; (b) At quarter span; (c) At mid span

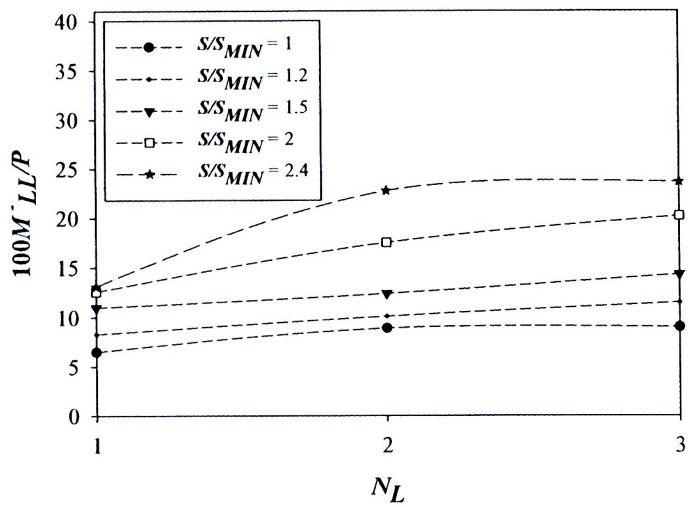

(c) At mid span

Figure 5.3 Variation of M^{-}_{LL}/P with respect to N_L: (a) At support; (b) At quarter span; (c) At mid span

5.3 Effects of Present Parameters on M^{+}_{LL}

This section presents the effects of influential parameters on M^{+}_{LL}/P. Note that only load case of N_L = 1 is considered herein according to the reason discussed in subsection 4.5.1 of Chapter 4. In this way, the numbers of N_L and N_G have insignificant effect on M^{+}_{LL}. The critical M^{+}_{LL} can obtain when the bridge with N_G = 3 is selected for each value of S (Cao, 1996). The numerical results of M^{+}_{LL}/P with respect to the considered parameters are pointed out as follows:

5.3.1 Effect of Span Length and Interval Diaphragm

For positive moments, the different in flexural rigidity of the girders in longitudinal direction can cause the variation of M^{+}_{LL} in general. Theoretically, the more flexible girders result in the higher M^{+}_{LL}. Actually, the bridge deck with more rigid girders and tied with higher number of interval diaphragms can cause in the decreasing of M^{+}_{LL}. When longer bridges are used, the stiffer girders are required in general. This will result in lower M^{+}_{LL}. To examine the effect of L solely, however, the same series size of the girders has been considered in this study.

In most bridge design and construction, interval diaphragms are intended to tie girders together to facilitate construction and maintenance, transfer lateral loads and improve traffic load distributions. Therefore, this element may be one of the important structural elements for live load distributions and bridge load capacities. However, in the calculation of load distribution and capacity verification, researches for example, Westergaard (1930) and Cao (1996) and many codes of recommendations exclude the presence of interval diaphragms in the model. As a result, in the Strip Width model it is a common practice to abandon the interval diaphragms and any other related diaphragms. Accordingly, this reason may lead to unrealistic prediction of M^{+}_{LL}.

As the reasons mentioned above, this subsection intents to investigate the effects of bridge span (***L***) and interval diaphragm on M^{+}_{LL}. For simplicity, the dimensionless parameter ***L/L_{MIN}*** where L_{MIN} stands for the minimum bridge span length of 15 m (50 ft) is used. The variations of M^{+}_{LL}/P with respect to L/L_{MIN} are showed in Figure 5.4.

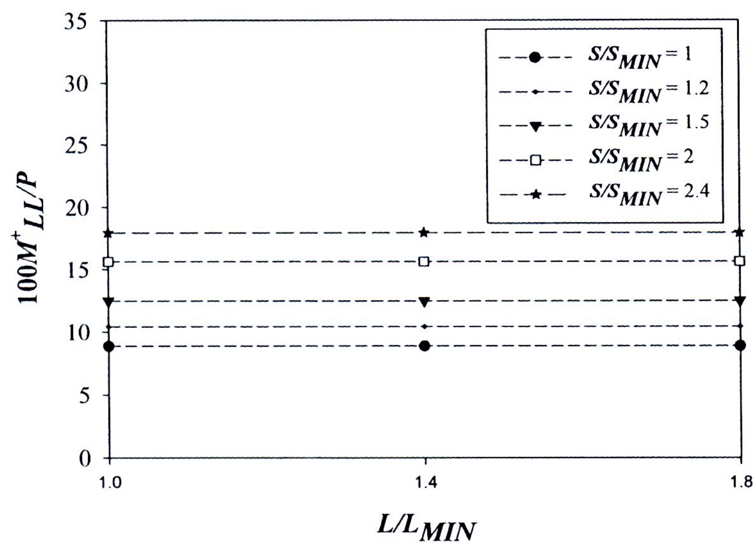

Without and with interval diaphragm

(a) At support

Figure 5.4 Variation of M^{+}_{LL}/P with respect to L/L_{MIN} (excluding ***m*** factor): (a) At support; (b) At quarter span; (c) At mid span

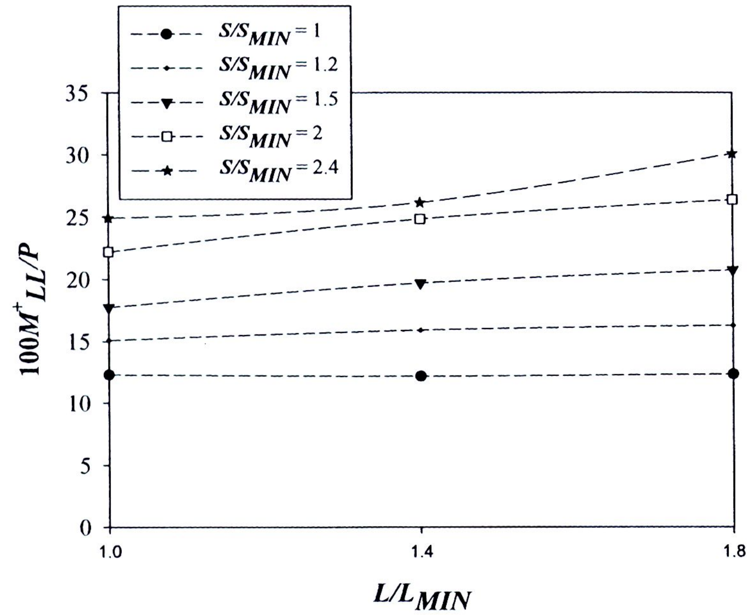

Without interval diaphragm

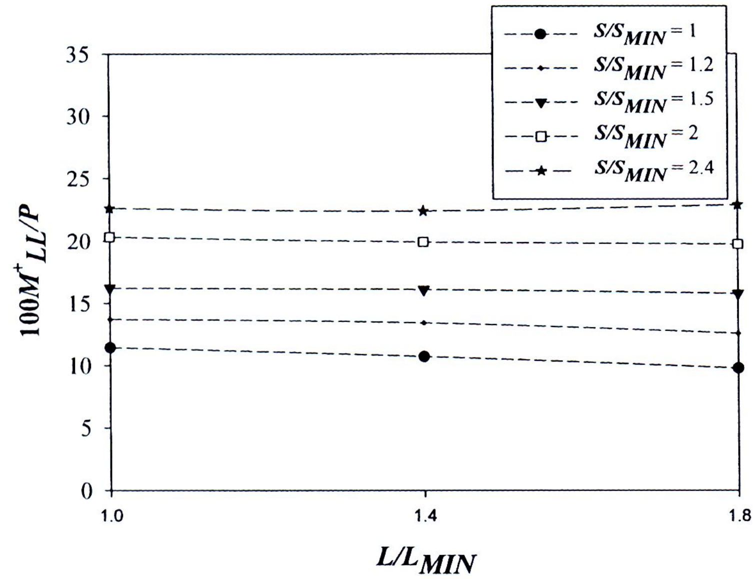

With interval diaphragm

(b) At quarter span

Figure 5.4 (Con't) Variation of M^{+}_{LL} /***P*** with respect to ***L/L$_{MIN}$*** (excluding ***m*** factor): (a) At support; (b) At quarter span; (c) At mid span

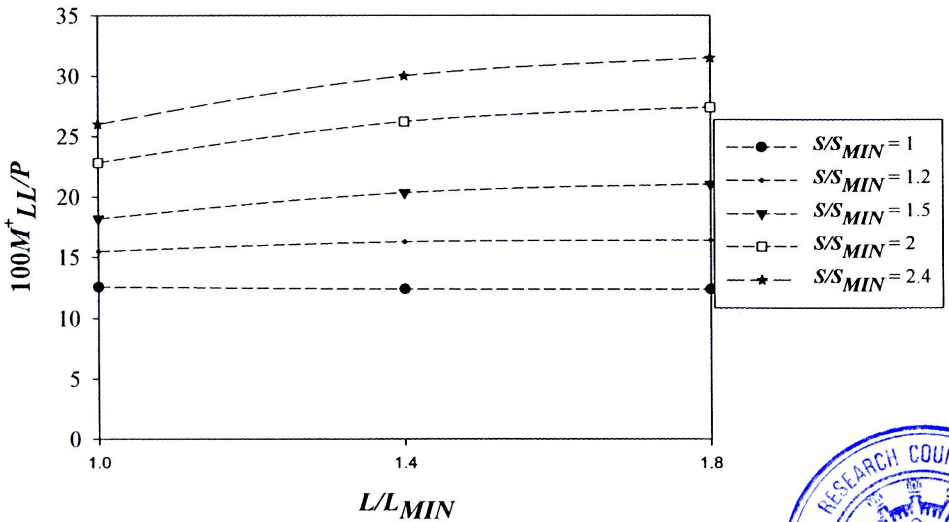

Without interval diaphragm

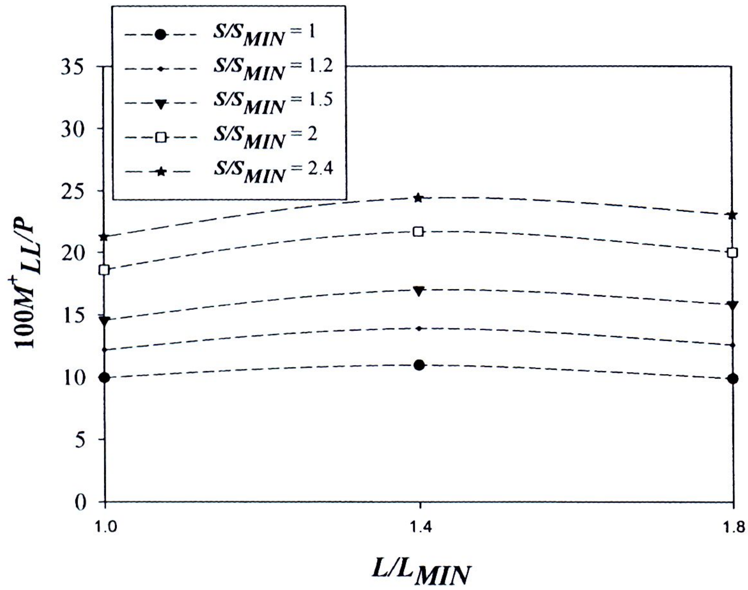

With interval diaphragm

(c) At mid span

Figure 5.4 (Con't) Variation of $M^+_{LL}/\boldsymbol{P}$ with respect to $\boldsymbol{L/L_{MIN}}$ (excluding $\boldsymbol{m}$ factor): (a) At support; (b) At quarter span; (c) At mid span

It has been observed in Figure 5.4 (a) that at the support the effect of L and interval diaphragm appears to be insignificant since they always give the same results of M^+_{LL} even if the bridges with or without interval diaphragms are considered or not. At the quarter and mid span, the effect of interval diaphragm can be observed. In case of the bridge without interval diaphragms, when $\boldsymbol{L/L_{MIN}}$ increases, $M^+_{LL}/\boldsymbol{P}$ rises in general. Conversely, when the bridge with interval diaphragms is used, the effect of $\boldsymbol{L}$ appears to be insignificant and can be negligible as shown in Figure 5.4 (b) and (c). For the reasons mentioned above, the effect of $\boldsymbol{L}$ will not be considered for the proposed formulas at the quarter and mid span including interval diaphragms and at the support.

5.3.2 Effect of Spacing of Girders

Figure 5.5 shows the typical effects of a dimensionless $\boldsymbol{S/S_{MIN}}$ on $M_{LL}^{+}/\boldsymbol{P}$ when the end diaphragms and with/without interval diaphragm are considered along locations of different $\boldsymbol{y}$. The numerical results indicate that $\boldsymbol{S/S_{MIN}}$ has significant influence on $M_{LL}^{+}/\boldsymbol{P}$: as $\boldsymbol{S/S_{MIN}}$ becomes larger, $M_{LL}^{+}/\boldsymbol{P}$ increases in general, especially either at the quarter or mid span regions without interval diaphragm.

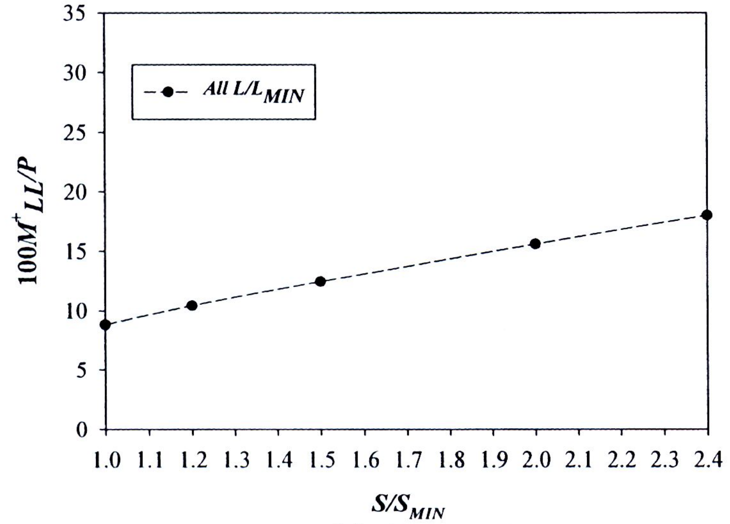

(a) At support

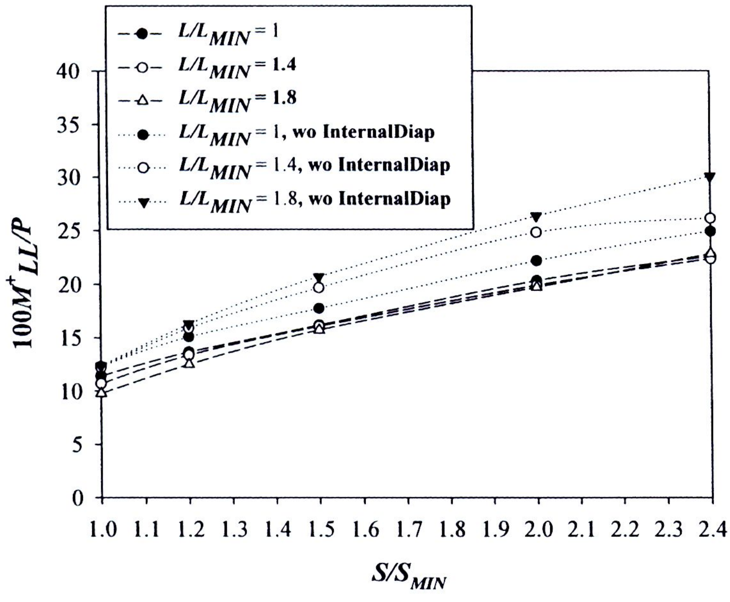

(b) At quarter span

Figure 5.5 Variation of $M_{LL}^{+}/\boldsymbol{P}$ with respect to $\boldsymbol{S/S_{MIN}}$ (excluding $\boldsymbol{m}$ factor): (a) At support; (b) At quarter span; (c) At mid span

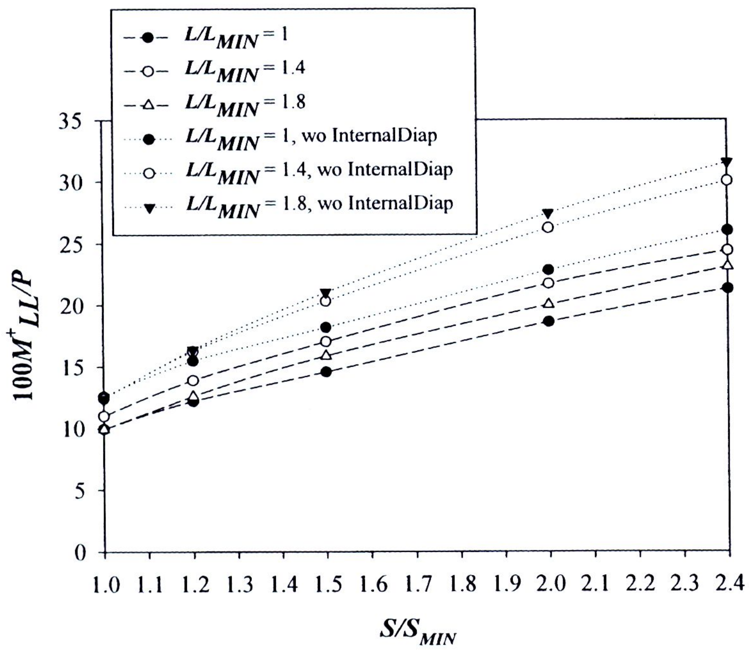

(c) At mid span

Figure 5.5 (Con't) Variation of M^{+}_{LL}/P with respect to S/S_{MIN} (excluding m factor): (a) At support; (b) At quarter span; (c) At mid span

In addition to subsection 5.3.1, it should be also noted that when the interval diaphragms are existing, the effect of L is relatively small as shown in Figure 5.5 (b). It has been also observed both in Figure 5.5 (b) and (c) that when $S/S_{MIN} \leq 1.2$, the effect of L is small for the bridge without interval diaphragms considered.

At this time, the numerical results also indicate that the absence and presence of interval diaphragms can cause the variation of M^{+}_{LL} as noticed in Figure 5.5 (b) and (c). Besides, M^{+}_{LL} due to the bridge with L either equal to 15 m (50 ft) or 21 m (70 ft) appears to be critical if interval diaphragms are excluded. In section 5.5, one proposed formula will be then presented at the quarter with interval diaphragm since the effect of L will not be considered. Whereas two proposed formulas will be presented at the quarter span without interval diaphragm for upper (L = 21 m (70 ft)) and lower bounds (L = 15 m (50 ft)). For the mid span, totally two formulas will be proposed by the same manner.

5.3.3 Effect of Loading Location

As shown in Figure 5.6, the location along bridge span denoted by the parameter y has a significant influence on M^{+}_{LL}/P for large S/S_{MIN} ($S/S_{MIN} \geq 1.5$). Nevertheless, the effect of y appears to be insignificant when the value of S/S_{MIN} is equal to 1. It should be also noted that at either the quarter or mid span, the magnitude of M^{+}_{LL}/P tends to be constant.

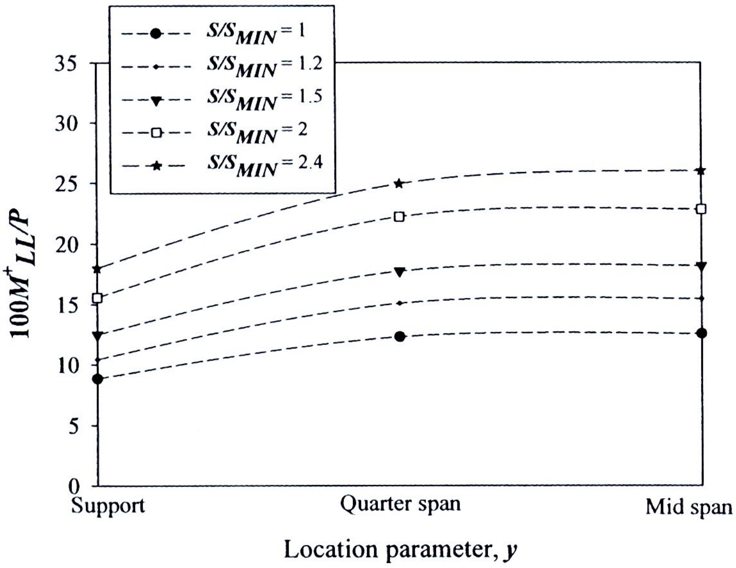

(a) L/L_{MIN} = 1

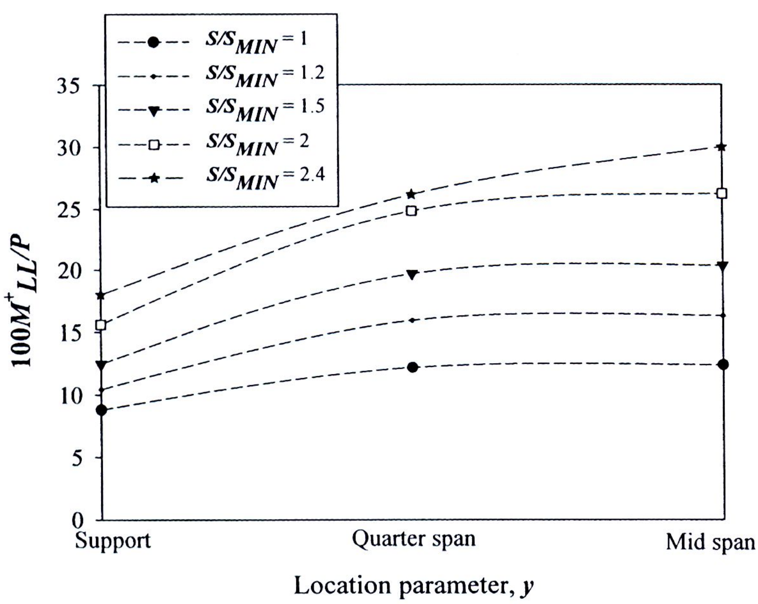

(b) L/L_{MIN} = 1.4

Figure 5.6 Variation of M^{+}_{LL}/P with respect to y (without interval diaphragm): (a) L/L_{MIN} = 1; (b) L/L_{MIN} = 1.4; (c) L/L_{MIN} = 1.8

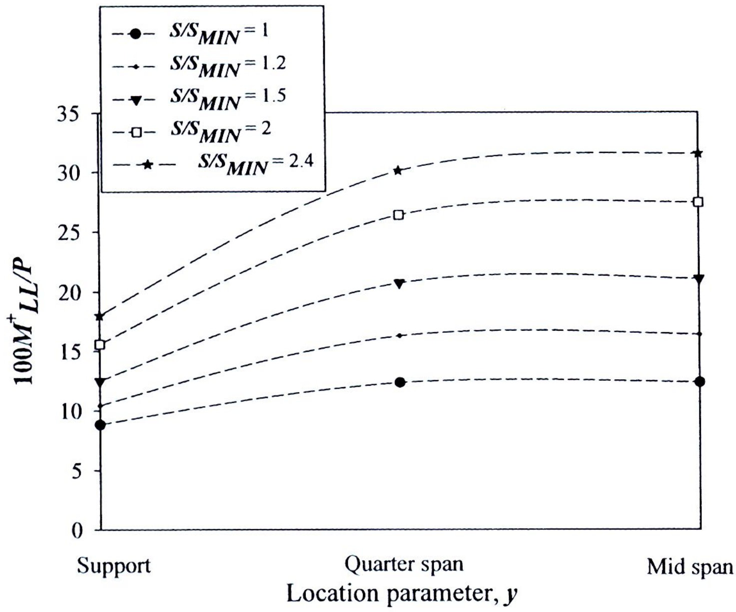

(c) L/L_{MIN} = 1.8

Figure 5.6 (Con't) Variation of M^+_{LL}/P with respect to y (without interval diaphragm): (a) L/L_{MIN} = 1; (b) L/L_{MIN} = 1.4; (c) L/L_{MIN} = 1.8

5.4 Comparisons of M_{LL}

At this time, M_{LL}/P (M^-_{LL}/P and M^+_{LL}/P) calculated by the present study are compared against other methods. The comparison of M^-_{LL}/P and M^+_{LL}/P are subsequently shown in subsection 5.4.1 and 5.4.2. In view of the design aspect, it should be noticed from the comparison results that the present selective M^-_{LL}/P (the critical value) can be used for the critical design value of slab moment at the support while the present selective M^+_{LL}/P can be used for the critical design value of the slab moment at quarter and mid span.

5.4.1 Comparison of M^-_{LL}

Table 5.1 (a), (b) and (c) show the comparison of M^-_{LL}/P for various values of S/S_{MIN} at the support, quarter span and mid span, respectively. By applying multiple presence factors m (according to AASHTO recommendations), the critical values of present M^-_{LL}/P (the highest one due to N_L = 1, 2 and 3) for each S/S_{MIN} can be obtained and stand for the present selective M^-_{LL}/P. In this study, those selective M^-_{LL}/P will be used as the acceptable results in the evaluation of M^-_{LL}/P due to the present study. The numerical percentage discrepancies with respect to present selective M^-_{LL}/P are also present in Table 5.1.

Table 5.1 M^-_{LL} ***/P*** due to present study and literature including ***m*** and a continuity factor: (a) At support; (b) At quarter span; (c) At mid span

(a) At support

Approach	M^-_{LL}/P									
	S/S_{min} = 1	% Diff	S/S_{min} = 1.2	% Diff	S/S_{min} = 1.5	% Diff	S/S_{min} = 2	% Diff	S/S_{min} = 2.4	% Diff
Present FEA: N_L = 1 (including *m* = 1.20)	0.110*	0	0.156*	0	0.204*	0	0.300	-5	0.326	-17
Present FEA: N_L = 2 (including *m* = 1.00)	0.094	-15	0.135	-13	0.192	-6	0.317*	0	0.391*	0
Present FEA: N_L = 3 (including *m* = 0.85)	0.081	-27	0.119	-24	0.165	-19	0.292	-8	0.335	-14
Westergaard	0.185	68	0.201	29	0.219	7	0.241	-24	0.254	-35
Cao and Shing	0.215	95	0.215	38	0.215	5	0.215	-32	0.215	-45
BD 81/02	0.198	79	0.189	21	0.177	-13	0.155	-51	0.138	-65
AASHTO Standards Method	0.175	59	0.200	28	0.238	17	0.300	-5	0.350	-10
AASHTO Strip Method [Table A4-1]	0.148	34	0.201	29	0.260	28	0.325	3	0.441	13
AASHTO Empirical Method (*0.380* mm^2/mm)	0.258	134	0.258	65	0.258	26	0.258	-19	0.258	-34
CHBDC	0.242	119	0.242	55	0.242	19	0.242	-24	0.242	-38
Cracking Moment	0.363	229	0.363	133	0.363	78	0.363	15	0.363	-7

* Used for the selective value of present FEA

(b) At quarter span

Approach	M^-_{LL}/P									
	S/S_{min} = 1	% Diff	S/S_{min} = 1.2	% Diff	S/S_{min} = 1.5	% Diff	S/S_{min} = 2	% Diff	S/S_{min} = 2.4	% Diff
Present FEA: N_L = 1 (including *m* = 1.20)	0.072	-2	0.108*	0	0.132*	0	0.169	-13	0.169	-19
Present FEA: N_L = 2 (including *m* = 1.00)	0.071	-3	0.100	-7	0.125	-5	0.194*	0	0.210*	0
Present FEA: N_L = 3 (including *m* = 0.85)	0.073*	0	0.093	-14	0.128	-3	0.190	-2	0.195	-7
Westergaard	0.185	153	0.201	86	0.219	66	0.241	24	0.254	21
Cao and Shing	0.160	118	0.160	49	0.164	24	0.171	-12	0.177	-16
BD 81/02	0.198	171	0.189	75	0.177	34	0.155	-20	0.138	-34
AASHTO Standards Method	0.175	139	0.200	85	0.238	80	0.300	55	0.350	67
AASHTO Strip Method [Table A4-1]	0.148	103	0.201	86	0.260	97	0.325	68	0.441	110
AASHTO Empirical Method (*0.380* mm^2/mm)	0.258	253	0.258	139	0.258	95	0.258	33	0.258	23
CHBDC	0.242	231	0.242	124	0.242	83	0.242	25	0.242	15
Cracking Moment	0.363	397	0.363	237	0.363	175	0.363	87	0.363	73

* Used for the selective value of present FEA

Table 5.1 M_{LL}^{-}/P due to present study and literature including m and a continuity factor: (a) At support; (b) At quarter span; (c) At mid span (Con't)

(c) At mid span

Approach	M_{LL}^{-}/P									
	S/S_{min} = 1	% Diff	S/S_{min} = 1.2	% Diff	S/S_{min} = 1.5	% Diff	S/S_{min} = 2	% Diff	S/S_{min} = 2.4	% Diff
Present FEA: N_L = 1 (including m = 1.20)	0.078	-12	0.100	-1	0.132*	0	0.156	-11	0.158	-31
Present FEA: N_L = 2 (including m = 1.00)	0.089*	0	0.101*	0	0.124	-6	0.175*	0	0.228*	0
Present FEA: N_L = 3 (including m = 0.85)	0.077	-14	0.098	-3	0.122	-8	0.172	-2	0.201	-12
Westergaard	0.185	108	0.201	99	0.219	66	0.241	38	0.254	12
Cao and Shing	0.137	54	0.138	37	0.143	8	0.153	-13	0.162	-29
BD 81/02	0.198	122	0.189	88	0.177	34	0.155	-11	0.138	-39
AASHTO Standards Method	0.175	97	0.200	98	0.238	80	0.300	71	0.350	54
AASHTO Strip Method [Table A4-1]	0.148	67	0.201	99	0.260	97	0.325	86	0.441	94
AASHTO Empirical Method (*0.380* mm^2/mm)	0.258	190	0.258	155	0.258	96	0.258	47	0.258	13
CHBDC	0.242	172	0.242	140	0.242	83	0.242	38	0.242	6
Cracking Moment	0.363	308	0.363	260	0.363	175	0.363	108	0.363	60

* Used for the selective value of present FEA

It appears that the variation of M_{LL}^{-}/P can be clearly observed among the different approaches. In particular, the present selective M_{LL}^{-}/P becomes minimum when S/S_{MIN} $\leq$ 1.2 and 1.5 in case of at the support (Table 5.1 (a)) and at quarter and mid span (Table 5.1 (b) and (c)), respectively. That is to say, M_{LL}^{-}/P due to the literature trends to be conservative when S/S_{MIN} becomes smaller than 1.5. As compared with the AASHTO Empirical Method (AASHTO, 2004), the maximum discrepancies of 134% (Table 5.1 (a)), 253% (Table 5.1 (b)) and 190% (Table 5.1 (c)) can be observed for the results at the support, quarter span and mid span, respectively. At the support region with widest S (S/S_{MIN} = 2.4), most approaches based on literature seem to give underestimated results compared with present FEA by inducing the maximum discrepancy of -65% in case of BD 81/02 [8] (Table 5.1 (a)). Only AASHTO Strip Method (AASHTO, 2004) gives more conservative results of 13% than these evaluated by present FEA for this S/S_{MIN}.

According to the present study, it has been suggested that current AASHTO design procedures should be noticeably conservative as they usually give quite larger M_{LL}^{-}/P than present FEA, especially for small S/S_{MIN}. The potential advantage of present FEA is that the amounts of slab reinforcements can be lower compared with the AASHTO counterpart. In particular, in case of quarter and mid span the slab reinforcements can be reduced in the range of 13% to 253%. It should be noted that both AASHTO Empirical Method (AASHTO, 2004) and CHBDC (2006) seem to provide comparable results as expected since both of them come from the same source (Ontario Bridge Code), which has a basic on the concept of arching action or compressive membrane action (CMA). The use of this design concept is important to note that the design of bridge deck is expected to be more economical than traditional designs. However, for the bridge with ***S/S$_{MIN}$*** $\leq$ 1.5, this seems to be disagreeable since those design codes (AASHTO Empirical Method 2004 and CHBDC 2006) always give the conservative results. Likewise, BD 81/02 (2005), which is based on the same concept of CMA seems to gives the conservative results when ***S/S$_{MIN}$*** is small.

In addition, it has been seen in Table 5.1 that the moment due to cracking can be probably used as an upper-bound tolerance. That is to say, this tolerance always stands for the maximum value of M^-_{LL} ***/P***. The present study has also revealed that when small *S/S$_{MIN}$* (***S/S$_{MIN}$*** $\leq$ 1.2) is selected the present selective M^-_{LL} ***/P*** may be applicable for the economic design since it always gives the minimum tolerance. For example, when compared with AASHTO Strip Method 2004, the amount of reinforcements based on present FEA in case of ***S/S$_{MIN}$*** = 1 should be reduced by 1.3, 2 and 1.7 times at the support (Table 5.1 (a)), quarter span (Table 5.1(b)) and mid span (Table 5.1(c)), respectively.

5.4.2 Comparison of M^+_{LL}

Table 5.2 (a) to (c.2) show the comparison of M^+_{LL} ***/P*** for various values of ***S/S$_{MIN}$*** at the support, quarter span and mid span. Like M^-_{LL} ***/P***, the critical values of present M^+_{LL} ***/P*** (the highest one) for each ***S/S$_{MIN}$*** can be determined and stand for the present selective M^+_{LL} ***/P***.

Table 5.2 M^+_{LL} **/P** due to present study and literature including m and a continuity factor (only a controlled case of $N_L = 1$ considered): (a) At support without and with interval diaphragm; (b.1) At quarter span without interval diaphragm; (b.2) At quarter span with interval diaphragm (using Max M^+_{LL}/P when $L/L_{MIN} = 1$); (c.1) At mid span without interval diaphragm; (c.2) At mid span with interval diaphragm

(a) At support without and with interval diaphragm

Approach	M^+_{LL}/P									
	S/S_{min} = 1	% Diff	S/S_{min} = 1.2	% Diff	S/S_{min} = 1.5	% Diff	S/S_{min} = 2	% Diff	S/S_{min} = 2.4	% Diff
Present FEA (including m = 1.20)	0.106*	0	0.125*	0	0.150*	0	0.188*	0	0.216*	0
Westergaard	0.185	74	0.201	60	0.219	46	0.241	28	0.254	18
Cao and Shing (Eq. (2.7))	0.183	73	0.196	56	0.213	42	0.234	25	0.247	14
BD 81/02	0.198	87	0.189	51	0.177	18	0.155	-17	0.138	-36
AASHTO Standards Method	0.175	65	0.200	60	0.238	58	0.300	60	0.350	62
AASHTO Strip Method [Table A4-1]	0.222	110	0.232	85	0.260	74	0.325	73	0.379	75
AASHTO Empirical Method (*0.380* mm^2/mm)	0.258	143	0.258	106	0.258	72	0.258	38	0.258	19
CHBDC	0.242	128	0.242	93	0.242	61	0.242	29	0.242	12
Cracking Moment	0.363	242	0.363	190	0.363	142	0.363	94	0.363	68

* Used for the selective value of present FEA

(b.1) At quarter span without interval diaphragm

Approach	M^+_{LL}/P									
	S/S_{min} = 1	% Diff	S/S_{min} = 1.2	% Diff	S/S_{min} = 1.5	% Diff	S/S_{min} = 2	% Diff	S/S_{min} = 2.4	% Diff
Present FEA L/L_{MIN} = 1 (including m = 1.20)	0.148	0	0.181	-7	0.213	-14	0.267	-16	0.299	-17
Present FEA L/L_{MIN} = 1.4 (including m = 1.20)	0.146	-1	0.191	-2	0.236	-5	0.298	-6	0.314	-13
Present FEA L/L_{MIN} = 1.8 (including m = 1.20)	0.148*	0	0.195*	0	0.249*	0	0.316*	0	0.361*	0
Westergaard	0.185	25	0.201	3	0.219	-12	0.241	-24	0.254	-30
Cao and Shing (Eq. (2.7))	0.183	24	0.196	0	0.213	-14	0.234	-26	0.247	-32
BD 81/02	0.198	34	0.189	-3	0.177	-29	0.155	-51	0.138	-62
AASHTO Standards Method	0.175	18	0.200	2	0.238	-4	0.300	-5	0.350	-3
AASHTO Strip Method [Table A4-1]	0.222	50	0.232	19	0.260	5	0.325	3	0.379	5
AASHTO Empirical Method (*0.380* mm^2/mm)	0.258	74	0.258	32	0.258	4	0.258	-18	0.258	-28
CHBDC	0.242	63	0.242	24	0.242	-3	0.242	-24	0.242	-33
Cracking Moment	0.363	145	0.363	86	0.363	46	0.363	15	0.363	1

* Used for the selective value of present FEA

Table 5.2 M^+_{LL} **/P** due to present study and literature including m and a continuity factor (only a controlled case of $N_L = 1$ considered): (a) At support without and with interval diaphragm; (b.1) At quarter span without interval diaphragm; (b.2) At quarter span with interval diaphragm (using Max M^+_{LL} **/P** when $L/L_{MIN} = 1$); (c.1) At mid span without interval diaphragm; (c.2) At mid span with interval diaphragm (Con't)

(b.2) At quarter span with interval diaphragm (using Max M^+_{LL} **/P** when $L/L_{MIN} = 1$)

Approach	M^+_{LL}/P									
	S/S_{min} = 1	% Diff	S/S_{min} = 1.2	% Diff	S/S_{min} = 1.5	% Diff	S/S_{min} = 2	% Diff	S/S_{min} = 2.4	% Diff
Present FEA L/L_{MIN} = 1 (including m = 1.20)	0.114*	0	0.137*	0	0.162*	0	0.204*	0	0.271*	0
Westergaard	0.185	62	0.201	47	0.219	35	0.241	18	0.269	-1
Cao and Shing (Eq. (2.7))	0.183	61	0.196	43	0.213	31	0.234	15	0.274	1
BD 81/02	0.198	74	0.189	38	0.177	9	0.155	-24	0.138	-49
AASHTO Standards Method	0.175	54	0.200	46	0.238	47	0.300	47	0.350	29
AASHTO Strip Method [Table A4-1]	0.222	95	0.232	69	0.260	61	0.325	59	0.379	40
AASHTO Empirical Method (*0.380* mm^2/mm)	0.258	126	0.258	88	0.258	59	0.258	26	0.258	-5
CHBDC	0.242	112	0.242	77	0.242	49	0.242	19	0.242	-11
Cracking Moment	0.363	219	0.363	165	0.363	124	0.363	78	0.363	34

* Used for the selective value of present FEA

(c.1) At mid span without interval diaphragm

Approach	M^+_{LL}/P									
	S/S_{min} = 1	% Diff	S/S_{min} = 1.2	% Diff	S/S_{min} = 1.5	% Diff	S/S_{min} = 2	% Diff	S/S_{min} = 2.4	% Diff
Present FEA L/L_{MIN} = 1 (including m = 1.20)	0.151*	0	0.186	-6	0.218	-14	0.274	-17	0.312	-17
Present FEA L/L_{MIN} = 1.4 (including m = 1.20)	0.149	-1	0.195	-1	0.244	-3	0.315	-4	0.354	-6
Present FEA L/L_{MIN} = 1.8 (including m = 1.20)	0.148	-2	0.197*	0	0.252*	0	0.329*	0	0.378*	0
Westergaard	0.185	23	0.201	2	0.219	-13	0.241	-27	0.254	-33
Cao and Shing (Eq. (2.7))	0.183	21	0.196	0	0.213	-16	0.234	-29	0.247	-35
BD 81/02	0.198	31	0.189	-4	0.177	-30	0.155	-53	0.138	-63
AASHTO Standards Method	0.175	16	0.200	2	0.238	-6	0.300	-9	0.350	-7
AASHTO Strip Method [Table A4-1]	0.222	48	0.232	18	0.260	3	0.325	-1	0.379	0.25
AASHTO Empirical Method (*0.380* mm^2/mm)	0.258	71	0.258	31	0.258	2	0.258	-22	0.258	-32
CHBDC	0.242	61	0.242	23	0.242	-4	0.242	-26	0.242	-36
Cracking Moment	0.363	141	0.363	85	0.363	44	0.363	11	0.363	-4

* Used for the selective value of present FEA

Table 5.2 M_{LL}^{+}/P due to present study and literature including m and a continuity factor (only a controlled case of $N_L = 1$ considered): (a) At support without and with interval diaphragm; (b.1) At quarter span without interval diaphragm; (b.2) At quarter span with interval diaphragm (using Max M_{LL}^{+}/P when $L/L_{MIN} = 1$); (c.1) At mid span without interval diaphragm; (c.2) At mid span with interval diaphragm (Con't)

(c.2) At mid span with interval diaphragm

Approach	M_{LL}^{+}/P									
	S/S_{min} = 1	% Diff	S/S_{min} = 1.2	% Diff	S/S_{min} = 1.5	% Diff	S/S_{min} = 2	% Diff	S/S_{min} = 2.4	% Diff
Present FEA (LowerBound) L/L_{MIN} = 1 (including m = 1.20)	0.119	-10	0.146	-12	0.175	-14	0.223	-14	0.256	-13
Present FEA (UpperBound) L/L_{MIN} = 1.4 (including m = 1.20)	0.132*	0	0.167*	0	0.204*	0	0.261 *	0	0.293 *	0
Present FEA L/L_{MIN} = 1.8 (including m = 1.20)	0.119	-10	0.151	-9	0.191	-7	0.240	-8	0.277	-5
Westergaard	0.185	40	0.201	21	0.219	7	0.241	-8	0.254	-13
Cao and Shing (Eq. (2.7))	0.183	39	0.196	18	0.213	4	0.234	-10	0.247	-16
BD 81/02	0.198	50	0.189	14	0.177	-13	0.155	-40	0.138	-53
AASHTO Standards Method	0.175	33	0.200	20	0.238	16	0.300	15	0.350	20
AASHTO Strip Method [Table A4-1]	0.222	69	0.232	39	0.260	27	0.325	25	0.379	29
AASHTO Empirical Method (*0.380* mm^2/mm)	0.258	96	0.258	55	0.258	26	0.258	-1	0.258	-12
CHBDC	0.242	84	0.242	45	0.242	18	0.242	-7	0.242	-17
Cracking Moment	0.363	176	0.363	118	0.363	78	0.363	39	0.363	24

* Used for the selective value of present FEA

It has been seen in Table 5.2 that M_{LL}^{+}/P due to literature appears to be conservative for most values of S/S_{MIN}. To be specific, at the support most of them are conservative except in case of BD 81/02 with $S/S_{MIN} \geq 2$ as shown in Table 5.2 (a). However, in case of quarter span and mid span for the bridge including the interval diaphragm most of them become conservative when $S/S_{MIN} \leq 1.5$ (Table 5.2 (b.2) and (c.2)). Reversely, most of the present FEA results seem to be conservative when $S/S_{MIN} \geq 1.5$ for the bridge excluding the interval diaphragm (Table 5.2 (b.1) and (c.1)).

Based on the comparison result, it has been observed that current AASHTO design procedures are noticeably conservative at the support since they usually give quite larger M_{LL}^{+}/P than present FEA about 19% to 143% for all values of S/S_{MIN}. The current AASHTO design procedure appears to give the comparable results with the present study when the bridge excluding interval diaphragms and $S/S_{MIN} \geq 1.5$ are considered.

For the reasons discussed above, it can be summarized that the interval diaphragm has no effect on M_{LL}^{+} **/P** at the support whereas it contributes some effects on M_{LL}^{+} **/P** at quarter and mid span. Like in case of M_{LL}^{-} **/P**, the moment due to cracking can be probably used as an upper-bound tolerance of M_{LL}^{+} **/P**.

5.5 Proposed Formulas

In this dissertation, there are two sets of the proposed formulas to determine the maximum bending moments M_{LL} for a practical range of a composite slab-over-girder deck. In particular, the empirical FEA-based formulas are developed herein to directly calculate the design M_{LL}^{+} and M_{LL}^{-}. Notably, the calculated M_{LL}^{+} and M_{LL}^{-} based on these formulas are excluded the factor of *IM* and multiple presence factors *m* (AASHTO, 2004). For the design values, M_{LL}^{+} and M_{LL}^{-} calculated according to the proposed formulas shall be multiplied by ***IM*** factor later. In order to establish the present FEA-based formulas, a curve fitting technique is applied to determine the relationship of the transverse moments M_{LL} in the slab with a reasonable R-square value of one. Based on present numerical results, the empirical formulas are proposed to directly evaluate M_{LL} for a practical deck slab design. In this process, a regression analysis is used to understand the statistical dependence of M_{LL} on the present considered parameters. The present proposed formulas can be expressed in term of $\boldsymbol{S/S_{MIN}}$ for each $\boldsymbol{N_L}$ as follows:

5.5.1 Design formulas of M_{LL}^{-}/P

For support region:

$$N_L = 1: M_{LL}^{-} = 0.01P\left[9.03 + 22.03\ln\left[S/S_{MIN}\right] - 0.84\left(\ln\left[S/S_{MIN}\right]\right)^2\right] \quad (5.1)$$

$$N_L = 2: M_{LL}^{-} = 0.01P\left[9.36 + 18.5\ln\left[S/S_{MIN}\right] + 18.17\left(\ln\left[S/S_{MIN}\right]\right)^2\right] \quad (5.2)$$

$$N_L = 3: M_{LL}^{-} = 0.01P\left[9.9 + 2.92\ln\left[S/S_{MIN}\right] + 80\left(\ln\left[S/S_{MIN}\right]\right)^2 - 50.68\left(\ln\left[S/S_{MIN}\right]\right)^3\right] \quad (5.3)$$

For quarter span:

$$N_L = 1: M_{LL}^{-} = 0.01P\left[6.12 + 13.88\ln\left[S/S_{MIN}\right] + \left(\ln\left[S/S_{MIN}\right]\right)^2 - 7.2\left(\ln\left[S/S_{MIN}\right]\right)^2\right] \quad (5.4)$$

$$N_L = 2: M_{LL}^{-} = 0.01P\left[7.33 + 5.85\ln\left[S/S_{MIN}\right] + 31.3\left(\ln\left[S/S_{MIN}\right]\right)^2 - 22.7\left(\ln\left[S/S_{MIN}\right]\right)^3\right] \quad (5.5)$$

$$N_L = 3: M_{LL}^{-} = 0.01P\left[8.73 + 0.12\ln\left[S/S_{MIN}\right] + 61.07\left(\ln\left[S/S_{MIN}\right]\right)^2 - 48.57\left(\ln\left[S/S_{MIN}\right]\right)^3\right] \quad (5.6)$$

For mid span:

$$N_L = 1: M_{LL}^- = 0.01P\left[6.36 + 13.65\ln\left[S/S_{MIN}\right] - 6.71\left(\ln\left[S/S_{MIN}\right]\right)^2\right] \quad (5.7)$$

$$N_L = 2: M_{LL}^- = 0.01P\left[9.04 + 1.84\ln\left[S/S_{MIN}\right] + 15.57\left(\ln\left[S/S_{MIN}\right]\right)^2\right] \quad (5.8)$$

$$N_L = 3: M_{LL}^- = 0.01P\left[9.04 + 11.22\ln\left[S/S_{MIN}\right] + 6.4\left(\ln\left[S/S_{MIN}\right]\right)^2\right] \quad (5.9)$$

It is noted that the above formulas are applicable in accordance with $\boldsymbol{L} \geq 15$ m (50 ft), $\boldsymbol{S_{MIN}} = 1.52$ m (5 ft), 1.52 m (5 ft) $\leq \boldsymbol{S} \leq 3.66$ m (12 ft), $\boldsymbol{H} \leq 0.91$ m (36 in), $1 \leq \boldsymbol{N_L} \leq 3$, $4 \leq \boldsymbol{N_G} \leq 7$ and $\boldsymbol{P} = 71.172$ kN (16 kips).

5.5.2 Design formulas of M_{LL}^+/P

Proposed formulas of $M_{LL}^+/\boldsymbol{P}$ are obtained from Figure 5.5 which is excluding ***m*** factor.

a) For support region

- Bridge without and with interval diaphragm:

$$M_{LL}^+ = 0.01P\left[8.878 + 7.63\ln\left[S/S_{MIN}\right] + 3.123\left(\ln\left[S/S_{MIN}\right]\right)^2\right] \quad (5.10)$$

b) For quarter span

- Bridge without interval diaphragm

$$L/L_{MIN} = 1: M_{LL}^+ = 0.01P\left[12.364 + 14.319\ln\left[S/S_{MIN}\right] - 2.521\left(\ln\left[S/S_{MIN}\right]\right)^2 + 3\left(\ln\left[S/S_{MIN}\right]\right)^3\right] \quad (5.11)$$

$$L/L_{MIN} = 1.4: M_{LL}^+ = 0.01P\left[12.27 + 17.088\ln\left[S/S_{MIN}\right] + 10.108\left(\ln\left[S/S_{MIN}\right]\right)^2 - 13.05\left(\ln\left[S/S_{MIN}\right]\right)^3\right] \quad (5.12)$$

$$L/L_{MIN} = 1.8: M_{LL}^+ = 0.01P\left[12.349 + 22.371\ln\left[S/S_{MIN}\right] - 5.707\left(\ln\left[S/S_{MIN}\right]\right)^2 + 3.737\left(\ln\left[S/S_{MIN}\right]\right)^3\right] \quad (5.13)$$

The integrated set of relationships in Eq. (5.11) to (5.13) for the maximum M_{LL}^+ can be proposed in terms of $\boldsymbol{S/S_{MIN}}$ and $\boldsymbol{L/L_{MIN}}$ as follows:

$$M_{LL}^+ = 0.01P\left\{A + B\ln\left[S/S_{MIN}\right] + C\left[\ln\left[S/S_{MIN}\right]\right]^2 + D\left[\ln\left[S/S_{MIN}\right]\right]^3\right\} \quad (5.14)$$

where

$$A = 13.356 - 1.533\frac{L}{L_{MIN}} + 0.541\left(\frac{L}{L_{MIN}}\right)^2 ; \; B = 18.395 - 11.933\frac{L}{L_{MIN}} + 7.856\left(\frac{L}{L_{MIN}}\right)^2 ;$$

$$C = -158.54 + 245\frac{L}{L_{MIN}} - 88.887\left(\frac{L}{L_{MIN}}\right)^2 ; \; D = 186.79 - 286.4\frac{L}{L_{MIN}} + 102.62\left(\frac{L}{L_{MIN}}\right)^2$$

- Bridge with interval diaphragm (using max. M_{LL}^{+} **/P** when $\boldsymbol{L/L_{MIN}} = 1$):

$$M_{LL}^{+} = 0.01P\left[10.716 + 14.935\ln\left[S/S_{MIN}\right] - 5.255\left(\ln\left[S/S_{MIN}\right]\right)^2 + 3.966\left(\ln\left[S/S_{MIN}\right]\right)^3\right] \quad (5.15)$$

c) For mid span

- Bridge without interval diaphragm:

$$L/L_{MIN} = 1: M_{LL}^{+} = 0.01P\left[12.614 + 15.712\ln\left[S/S_{MIN}\right] - 6.537\left(\ln\left[S/S_{MIN}\right]\right)^2 + 6.983\left(\ln\left[S/S_{MIN}\right]\right)^3\right] \quad (5.16)$$

$$L/L_{MIN} = 1.4: M_{LL}^{+} = 0.01P\left[12.418 + 21.207\ln\left[S/S_{MIN}\right] - 5.255\left(\ln\left[S/S_{MIN}\right]\right)^2 + 4.583\left(\ln\left[S/S_{MIN}\right]\right)^3\right] \quad (5.17)$$

$$L/L_{MIN} = 1.8: M_{LL}^{+} = 0.01P\left[12.38 + 21.881\ln\left[S/S_{MIN}\right] - 1.768\left(\ln\left[S/S_{MIN}\right]\right)^2 + 1.987\left(\ln\left[S/S_{MIN}\right]\right)^3\right] \quad (5.18)$$

The simplified set of relationships in Eq. (16) to (18) for the critical M_{LL}^{+} at mid span for the bridge without interval diaphragms can be mutually proposed in terms of $\boldsymbol{S/S_{MIN}}$ and $\boldsymbol{L/L_{MIN}}$ as follows:

$$M_{LL} = 0.01P\left\{A + B\ \ln\left[S/S_{MIN}\right] + C\ \left[\ln\left[S/S_{MIN}\right]\right]^2 + D\ \left[\ln\left[S/S_{MIN}\right]\right]^3\right\} \quad (5.19)$$

where

$$A = 13.795 - 1.675\frac{L}{L_{MIN}} + 0.494\left(\frac{L}{L_{MIN}}\right)^2 ; \; B = -19.117 + 50\frac{L}{L_{MIN}} - 15.066\left(\frac{L}{L_{MIN}}\right)^2 ;$$

$$C = -0.095 - 13.332\frac{L}{L_{MIN}} + 6.891\left(\frac{L}{L_{MIN}}\right)^2 ; \; D = 12.126 - 4.53\frac{L}{L_{MIN}} - 0.613\left(\frac{L}{L_{MIN}}\right)^2$$

- Bridge with interval diaphragm:

<u>Lower bounds</u>

$$L/L_{MIN} = 1: M_{LL} = 0.01P\left[10 + 11.445\ln\left[S/S_{MIN}\right] - 0.555\left(\ln\left[S/S_{MIN}\right]\right)^2 + 2.627\left(\ln\left[S/S_{MIN}\right]\right)^3\right] \quad (5.20)$$

<u>Upper bounds</u>

$$L/L_{MIN} = 1.4: M_{LL} = 0.01P\left[11.02 + 14.806\ln\left[S/S_{MIN}\right] + 1.187\left(\ln\left[S/S_{MIN}\right]\right)^2 - 0.684\left(\ln\left[S/S_{MIN}\right]\right)^3\right] \quad (5.21)$$

Likewise, the integrated set of relationships in Eq. (20) to (21) for the critical M^{+}_{LL} at mid span for the bridge with interval diaphragms can be proposed in terms of ***S/S$_{MIN}$*** and ***L/L$_{MIN}$*** as follows:

$$M_{LL} = 0.01P\left\{A + B\ \ln[S/S_{MIN}] + C\ [\ln[S/S_{MIN}]]^2 + D\ [\ln[S/S_{MIN}]]^3\right\} \quad (5.22)$$

where

$$A = 7.45 + 2.55\frac{L}{L_{MIN}};\ B = 3.043 + 8.403\frac{L}{L_{MIN}};\ C = -4.91 + 4.355\frac{L}{L_{MIN}};$$

$$D = 10.91 - 8.278\frac{L}{L_{MIN}}$$

It is noted that the above formulas are applicable in accordance with $S/L \leq 0.24$, $S/t \leq 18$, $1 \leq S/S_{MIN} \leq 2.4$ when $S_{MIN} = 1.52$ m (5 ft), $L/L_{MIN} \leq 1.8$ ($L_{MIN} = 15$ m (50 ft)), $H \leq 0.91$ m (36 in), $N_L \geq 1$ and $P = 71.172$ kN (16 kips).

5.6 Simple Closed Forms of M_{LL}

5.6.1 Design formulas of M_{LL}/P in terms of *S* and *N*

This section describes a simple method taking into account full composite action between deck and girder. To represent the based model of critical moments M^{+}_{LL} and M^{-}_{LL}, the loading patterns of moving trucks is considered herein. In general, the bridge deck is loaded in different vehicle patterns which may occur during a real traffic situation. The loading patterns of moving trucks in transverse direction can be expressed by a dimensionless ratio, ***N***, defined as follows:

$$N = \frac{N_L}{N_G} \quad (5.23)$$

where N_L is the number of transverse traffic lanes and N_G is the number of girders

According to previous design code of AASHTO Standard (2002), the variations of moment in slab over flexible girders have been provided by considering only a primary parameter ***S*** and magnitude of a wheel load ***P***. In addition, the parameter ***N*** seems to be less important since it was fixed to ***0.33*** in Cao's study and not mentioned in LRFD (AASHTO, 2004). It is noticeable that the analytical method by Cao (1996) gives good estimation when the girder spacing ***S*** is not large ($S < 3$ m or 10 ft) where the maximum M_{LL} can be evaluated due to one wheel load only (i.e. $N_L = 1$). However, to predict the values of M_{LL} more detailed, all effects of ***S***, ***y***, ***N*** and ***P*** are considered in the previous section. Once the different approaches are used, some discrepancies of M_{LL} can be clearly observed among the references and present study as discussed in section 5.4.

5.6.2 Formulation of Effective Strip Width

According to AASHTO design code, the transverse deck moments causing by transverse loadings in concrete bridge decks have been alternatively provided in form of the estimated strips width. This approach appears to be a useful way for the bridge deck design. At this time, this method may be applicable as a simplified tool during bridge design instead of using traditional AASHTO provisions. To facilitate this, a proposed strip width is developed so as to provide a simple mean for designers to perform the same as AASHTO strip method (2004). Based on the overview of a significant number of researches (Badaruddin, 1965; Bathe and Wilson, 1976; Beeby, 1978; Bakht and Jaeger, 1990; Bakht and Jaeger, 1992; Bakht and Lam, 2000; Barker and Puckett, 2007) over the past several decades about the M^+_{LL} design strip, the works of Westergaard and AASHTO strip method were presented to simplify the use of those methods. It should be noted that only AASHTO strip method is presented to simplify the M^-_{LL} design strip.

In general, it is always cost effective for the engineer to simplify the modeling approaches employed in order to estimate the structural responses of the components within the structure. Before the invention of digital computers, the effective strip width concept for the positive transverse moments in the deck slab system had been mentioned by AASHTO design methods (Table 4.6.2.1.3-1) and Westergaard (1930).

To be able to compute the effective strip width (B_E), a useful formula based on the classical simple beam theory is proposed. This formula is depended on the maximum M_{LL} per unit width of slab. By assuming that the moment is distributed uniformly over a certain width of a simple span slab in the direction of perpendicular to the span of the slabs $\boldsymbol{S}$, $\boldsymbol{B_E}$ can be defined below:

$$B_E = \frac{PS}{4M_{LL}} = \frac{0.25S}{M_{LL}/P} \tag{5.24}$$

where M_{LL} is the proposed design formulas of M^-_{LL} is M^+_{LL}

5.6.3 Formulation of Effective Strip Width: Current LRFD Formula

Based on the present numerical results, B_E can be calculated according to equation (5.24) for each $\boldsymbol{S}$. Note that these $\boldsymbol{B_E}$ are based on the results of bridges without and with the consideration of interval diaphragms. In order to establish the present FEA-based formulas, a curve fitting technique is used to determine the relationship between $\boldsymbol{B_E}$ and $\boldsymbol{S/S_{MIN}}$. Based on the present numerical results, Equations 5.25 to 5.28 are now proposed for $\boldsymbol{B_E}$ used to estimate the value of M_{LL} in different span region.

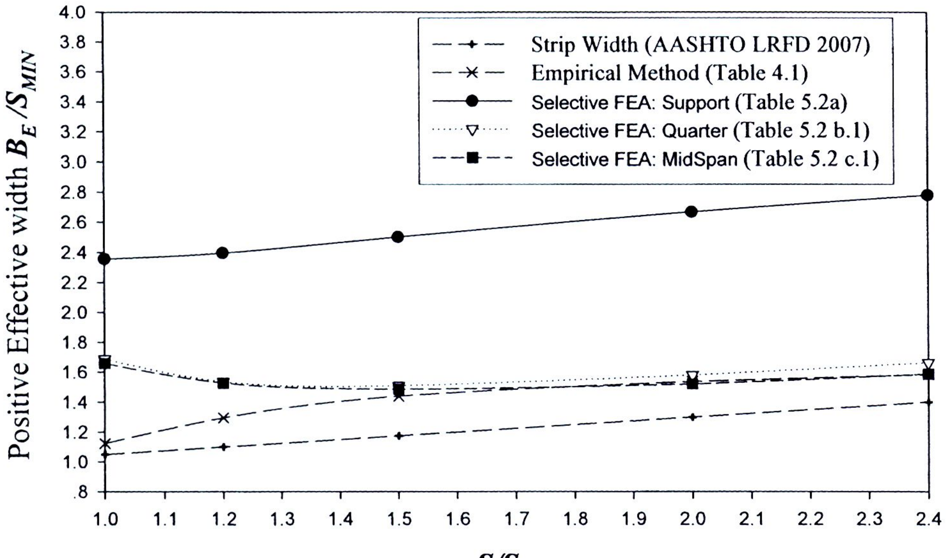

Without interval diaphragm

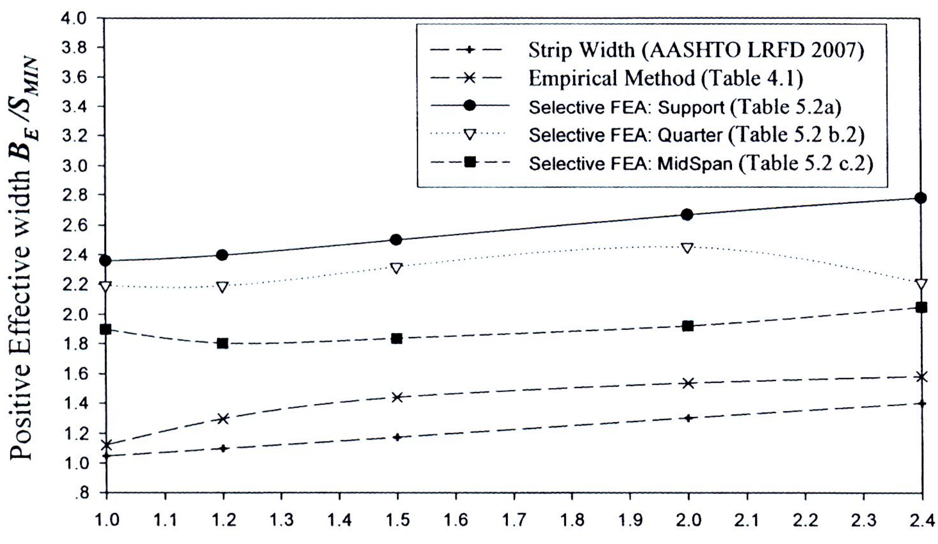

With interval diaphragm

(a) Variation of B_E/S_{MIN} for M^+_{LL} with respect to S/S_{MIN}

Figure 5.7 Comparison of proposed B_E/S_{MIN} and AASHTO methods: (a) Variation of B_E/S_{MIN} for M^+_{LL} with respect to S/S_{MIN}; (b) Variation of B_E/S_{MIN} for M^-_{LL} with respect to S/S_{MIN}

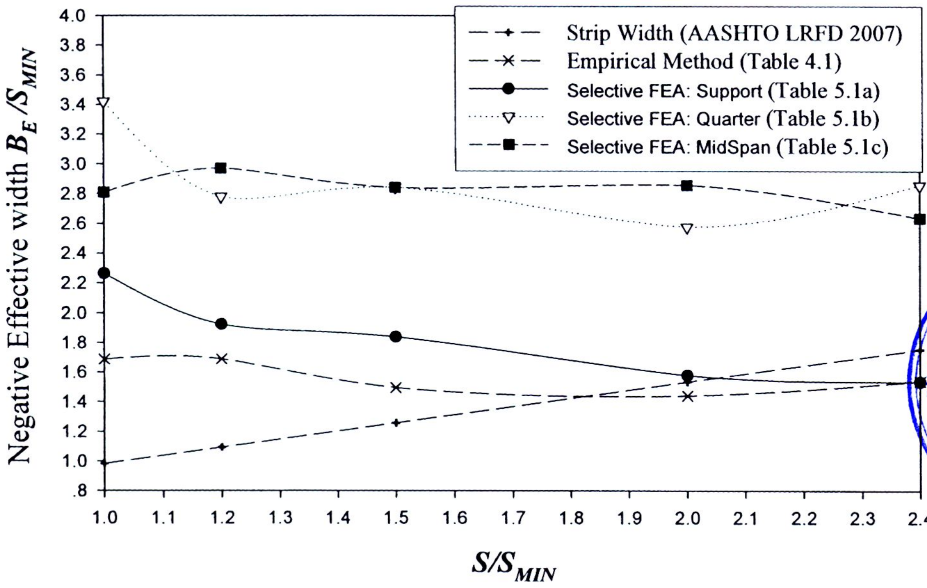

(b) Variation of B_E/S_{MIN} for M^-_{LL} with respect to S/S_{MIN}

Figure 5.7 (Con't) Comparison of proposed B_E/S_{MIN} and AASHTO methods:
(a) Variation of B_E/S_{MIN} for M^+_{LL} with respect to S/S_{MIN};
(b) Variation of B_E/S_{MIN} for M^-_{LL} with respect to S/S_{MIN}

Figure 5.7 shows the variation of B_E/S_{MIN} with respect to S/S_{MIN} for different locations along bridge span. It can be seen that as S/S_{MIN} increases ($S/S_{MIN} \geq 1.2$), B_E/S trends to decrease in general even though the different location along the span is considered. This is in accordance with the assumptions used by Westergaard (1930). Besides, it should be also noted that AASHTO procedures give rather smaller B_E/S_{MIN} for most cases. Based on the FEA analysis, the bridge with three girders under N_L = 1 always gives the maximum M^+_{LL} which is implied by the minimum value of B_E. In addition, it is apparent that B_E is usually minimum at the mid span section when the structural flexibility of bridge deck is largest. On the other hand, the maximum B_E can be observed when the bridge deck is rigidly restrained at the support.

For support region:

$$\text{For } M^-_{LL} : B_E = S_{MIN}\left[2.233 - 1.41\ln\left[S/S_{MIN}\right] + 0.7\left(\ln\left[S/S_{MIN}\right]\right)^2\right] \tag{5.25}$$

$$\text{For } M^+_{LL} : B_E = S_{MIN}\left[2.351 + 0.251\ln\left[S/S_{MIN}\right] + 0.277\left(\ln\left[S/S_{MIN}\right]\right)^2\right] \tag{5.26}$$

For other regions:

$$\text{For } M^-_{LL} : B_E = S_{MIN}\left[2.813 - 0.017\ln\left[S/S_{MIN}\right] - 0.267\left(\ln\left[S/S_{MIN}\right]\right)^2\right] \tag{5.27}$$

- Bridge without interval diaphragm:

$$\text{For } M_{LL}^{+}: B_E = S_{MIN}\left[1.65 - 0.72\ln\left[S/S_{MIN}\right] + 0.75\left(\ln\left[S/S_{MIN}\right]\right)^2\right] \quad (5.28a)$$

- Bridge with interval diaphragm:

$$\text{For } M_{LL}^{+}: B_E = S_{MIN}\left[1.887 - 0.48\ln\left[S/S_{MIN}\right] + 0.76\left(\ln\left[S/S_{MIN}\right]\right)^2\right] \quad (5.28b)$$

5.7 Effect of Dead Load of Bridge Deck

5.7.1 Slab Moment Due to Dead Load of Bridge Deck

The ultimate purpose in computing deflections due to self-weight of steel girder and slab is to produce a structure which will conform to the profile grade after the effects of immediate dead load deflection. In general, the deflection of slab increases when the bridge with wider ***S*** is used. This leads to the increment in both positive and negative slab moment due to dead load (M_{DL}^{+} and M_{DL}^{-}).

Unlike the influence of live loads that can be transient on the bridge deck slab, the analysis of M_{DL}^{+} and M_{DL}^{-} can be paid less attention. This should be due to the fact that dead loads of bridge deck are typically considered as a static load and represent a small fraction of the deck loads. Using a simplified approach to determine the deck dead load effects will result in a negligible difference in the total load effects (***DL*** + ***LL***). Traditionally, dead load positive and negative moments in the deck, except for the overhang, for a unit width strip of the deck can be calculated using the following formula:

$$M_{DL} = 0.80\, wS^2/C \quad (5.29)$$

where

M_{DL} = dead load positive or negative moment in the deck for a unit width strip (kN-m/m)

w = dead load per unit area of the deck (kN/m^2)

S = girder spacing (m)

C = constant, typically taken as 10 (the number of girders N_G = 3) or 12 (the number of girders, N_G = 4)

In case of bridge deck without camber, the trends of dead load slab moment can be seen from extending the models of field test of Fang et al. (1990) (see Figure 3.7) and it seems that the effect of girder flexibility can cause the variation of M_{DL}^{+} **/P** and M_{DL}^{-} **/P** as shown in Figure 5.8. To be specific, the magnitude of M_{DL}^{+} and M_{DL}^{-} calculated from the present FEA respectively increases and decreases when y approaches the mid span where the flexibility of the girder is high.

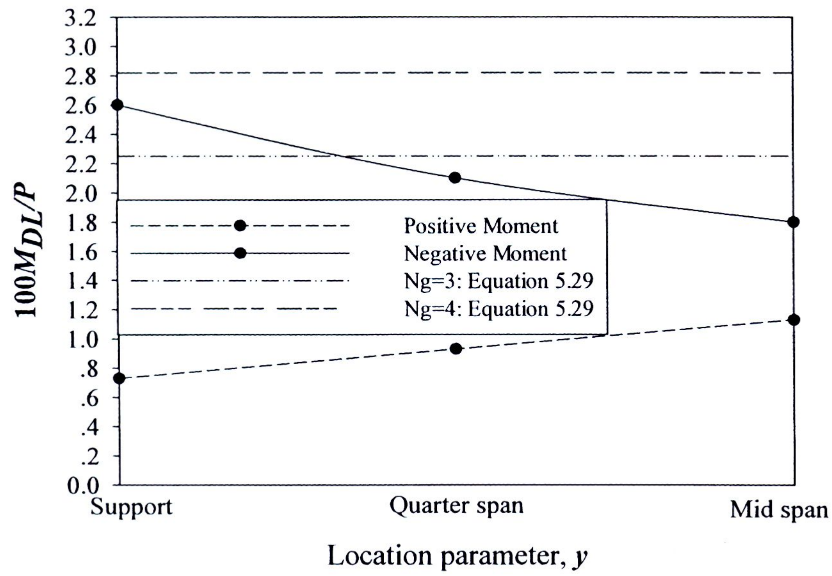

Figure 5.8 Variation of M_{DL}/P with respect to locations of span (S/S_{MIN}= 1.4)

In addition, the validation results also prove that the magnitude of M_{LL}^{-} at a specific loading position $y = L/3$ gives 6 and 12 times of magnitude of M_{DL}^{-} and M_{DL}^{+}, respectively.

5.7.2 Suggestion of Dead Load Slab Moments

Unlike live load design, the effect of self-weight of the bridge is taken into account for interior girders for negative dead load moment. The conservative design will be used for a basic deck thickness of 20 cm (8 in). The author suggests that C should be taken as 10 for any number of girders to stand for the conservative dead load deck slab (see Eq. 5.29).

It should be noted from Figure 5.9 that M_{DL} due to the present FEA always lay on the minimum lower bound. This minimum M_{DL}^{+} indicates an insignificant effect compared with M_{LL}. In particular, at the support, the variation of M_{DL}/P with respect to S/S_{MIN} can be proved that the magnitudes of M_{LL}^{+} and M_{LL}^{-} gives 3 to 9 and 6 to 9 times higher than M_{DL}, respectively, as illustrated in Figure 5.9.

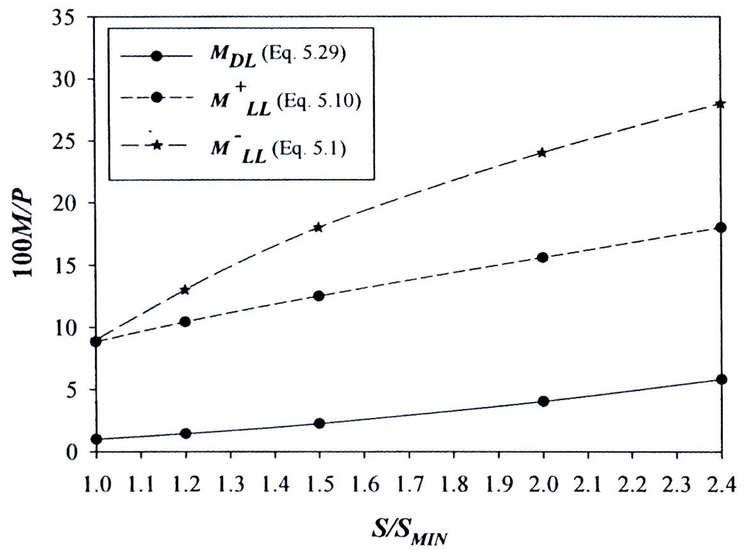

Figure 5.9 Comparision of M_{DL} with respect to M_{LL} at support (N_L = 1)

According to the trends of M_{DL} shown in Figure 5.9, the author suggests that the maximum magnitude of M^+_{DL} can be determined when interval diaphragms and slab camber (upward deflection) are excluded for the bridge with L/L_{MIN} = 1.8. To this end, it is not intended to determine the magnitudes of either M^+_{DL} or M^-_{DL} by the refined analysis since its magnitude calculated from the AASHTO formula (Eq. 5.29) should be governed the design moment due to dead load.

5.8 Reliability of the Proposed Formulas

The reliability of the proposed formulas is examined by comparing the present estimates with those obtained from a commercial design software, CSI Bridge. As an example application, the estimation of M^-_{LL} and M^+_{LL} according to the proposed formulas and FEA is conducted. By comparing M^-_{LL} and M^+_{LL} due to the proposed formulas with those evaluated from the software package, reliability of the proposed formulas is verified at this time. The verification is conducted for a 2-span continuous bridge design example as shown in Figure 5.10, which has a clear roadway width of 12.2 m (40 ft), ***L*** of 27.4 m (90 ft), ***S*** of 3.35 m (11 ft), N_G of 4, girder section of W40x215 and slab thickness of 0.216 m (8.5 in) with f_c' = 28 MPa (4000 psi). The comparison results between the two methods are made and presented as follows:

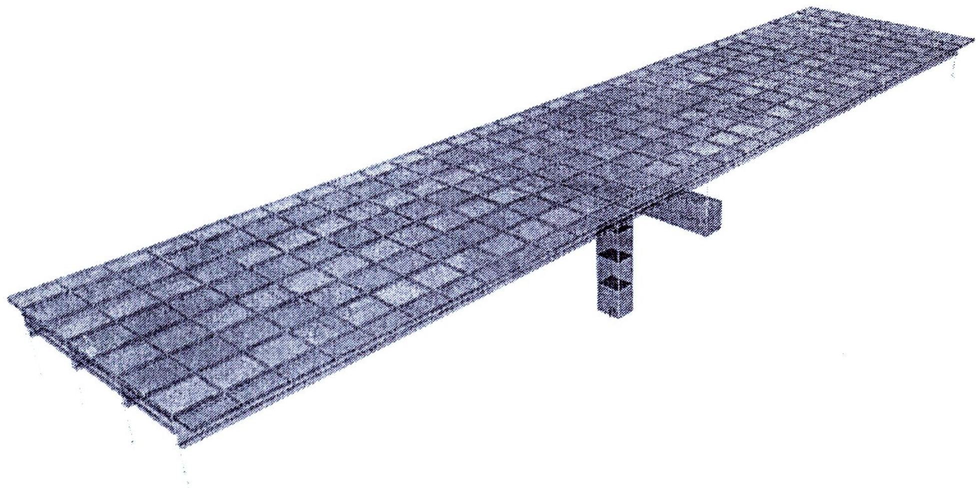

Figure 5.10 Bridge design example

5.8.1 Reliable Design of M_{LL}^{-}

Table 5.3 shows $M_{LL}^{-}/\boldsymbol{P}$ calculated from the proposed formulas together with the results obtained from a famous commercial bridge design software, CSI Bridge. $M_{LL}^{-}/\boldsymbol{P}$ for different locations of $\boldsymbol{y}$ and $\boldsymbol{N_L}$ are of interest. It has been observed that at the support reasonable agreement can be observed among the two methods (the discrepancy within the maximum of 8%). Although the proposed formulas tend to overestimate the results for all locations, such conservative values are supposed to be suitable for the design viewpoint.

Table 5.3 Reliability of $M_{LL}^{-}/\boldsymbol{P}$ calculated from proposed formulas

Approach	$M_{LL}^{-}/\boldsymbol{P}$			% Diff.		
	y			y		
	Support	Quarter span	Mid span	Support	Quarter span	Mid span
Software-based: $N_L = 1$	0.24	0.07	0.06	-	-	-
Software-based: $N_L = 2$	0.33	0.08	0.07	-	-	-
Software-based: $N_L = 3$	0.36	0.09	0.08	-	-	-
$N_L = 1$: Eq. 5.1, 5.4, 5.7	0.26	0.14	0.13	8	50	54
$N_L = 2$: Eq. 5.2, 5.5, 5.8	0.35	0.20	0.20	6	60	65
$N_L = 3$: Eq. 5.3, 5.6, 5.9	0.37	0.23	0.22	3	61	64

5.8.2 Reliable Design of M_{LL}^{+}

In relation to $M_{LL}^{+}/\boldsymbol{P}$ evaluation, the proposed formulas give the acceptable results compared with the design-software-based results for different location of $\boldsymbol{y}$ as shown in

Table 5.4. The comparison results show the discrepancy within the maximum of 18% between the two methods. Like $M_{LL}^{-}/\boldsymbol{P}$ evaluation, the proposed formulas give conservative results and should be used for the design values.

Table 5.4 Reliability of $M_{LL}^{+}/\boldsymbol{P}$ calculated from proposed formulas

Approach	$M_{LL}^{+}/\boldsymbol{P}$			% Diff.		
	y			*y*		
	Support	Quarter span	Mid span	Support	Quarter span	Mid span
Software-based: $\boldsymbol{L/L_{MIN}}$ = 1.8	0.16	0.23	0.26	-	-	-
Eq. 5.10, 5.14, 5.19: $\boldsymbol{L/L_{MIN}}$ = 1.8	0.17	0.28	0.30	6	18	13

5.9 Suggestion of Reinforcement Area in Deck Slab

In addition to designing the deck for dead and live loads at the strength limit state, the design specifications require checking the deck for the extreme event under the critical loading effect. The resistance factor at the extreme event limit state is taken as *1.0*. This signifies that at this level of loading, damage to the structural components is allowed and the goal is to prevent the collapse of any structural components. Once these limitations are satisfied, the design specifications give reinforcement ratios for both the longitudinal and transverse reinforcement for both layers of deck reinforcement. To determine the live load moment per unit width of the bridge, the total live load moment is calculated using the methods provided by the design codes. In lieu of this procedure, the present study gives the live load moment per unit width of the deck to be determined using Eq. 5.1 to 5.22. At this stage, the reinforcement determined in this section is based on the maximum M_{LL}^{-} and M_{LL}^{+} according to the proposed formulas as well as M_{DL}^{-} and M_{DL}^{+} as recommended in subsection 5.7.2.

The slab must be reinforced with four layers of reinforcement as shown in Figure 5.11. Reinforcement shall be located as close to the outside surfaces as permitted by cover requirements.

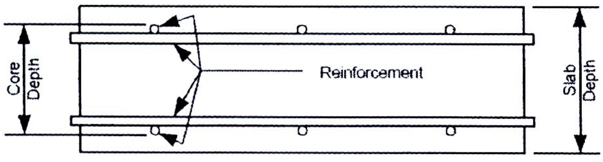

Figure 5.11 Design reinforcement section of slab

Note: Top Cover = 65 mm, Bottom Cover = 25 mm (Bottom of cast-in-place slabs)

According to AASHTO design procedure, reinforcement recommended by the Empirical Method (AASHTO 2007) can be determined as more convenient. The reinforcement shall be provided in each face of the slab with the outermost layers placed in the direction of the effective length. By this way, the minimum amount of reinforcement (As_{min}) shall be 0.570 mm^2/mm (0.27 in^2/ft) of steel for each bottom layer (about 0.28% reinforcement steel) and 0.380 mm^2/mm (0.18 in^2/ft) of steel for each top layer (about 0.19% reinforcement steel). To satisfy this design concept, the spacing of steel girders shall not exceed 450 mm. In general, reinforcing steel shall be Grade 420 or better. Typically, the traditional cross-sectional area of reinforcement bar showed in Table 5.5 is used.

Table 5.5 Typical reinforcing bar properties

Bar Size No.	Nominal Mass (kg/m)	Nominal Diameter (mm)	Nominal Area (mm^2)	Bar Size No.	Nominal Weight (lb/ft)	Nominal Diameter (in)	Nominal Area (in^2)
10	0.560	9.5	71	3	0.376	0.375	0.11
13	0.994	12.7	129	4	0.668	0.500	0.20
16	1.552	15.9	199	5	1.043	0.625	0.31
19	2.235	19.1	284	6	1.502	0.750	0.44
22	3.042	22.2	387	7	2.044	0.875	0.60
25	3.973	25.4	510	8	2.670	1.000	0.79
29	5.060	28.7	645	9	3.400	1.128	1.00
32	6.404	32.3	819	10	4.303	1.270	1.27
36	7.907	35.8	1006	11	5.313	1.410	1.56
43	11.380	43.0	1452	14	7.650	1.693	2.25
57	20.240	57.3	2581	18	13.600	2.257	4.00

Note: In general, No. 16 bars are widely used for main layers of for the deck slab for top and bottom mats

In recent years, fiber reinforced polymers (FRP) has been widely used for bridge construction throughout the world. In spite of their higher initial costs, the FRP prefer to possess advantage of an excellent durability over the conventional materials or reinforcing bars (Hyeong-Yeol Kim et al., 2006). This type of bridge deck is sometimes called the steel-free deck. Due to the durability problem, the lower amount of reinforcing bars used can result in the enhancement in deck slab durability. For this benefit, the minimum requirement of reinforcement may be preferred in some specific decks. In some situations, the obtained magnitude of the maximum M_{LL} due to the present study is governed by the temperature reinforcement in slab deck only. As a result, the minimum requirement of reinforcement area (A_{Smin}) in a deck slab may possibly follow the temperature reinforcement of 2.65 cm^2 per meter of surface (0.125 in^2 per foot) according to AASHTO Standard 2002 (about 0.20% reinforcement steel).

The ratio between the required reinforcement area (A_S) and A_{Smin} (A_S/A_{Smin}) for top and bottom mats based on the present FEA and AASHTO Strip Method can be determined using M_{LL} including the factors of impact ***IM*** (*1.33*) and *m* factors. Figures 5.12 and 5.13 respectively show A_S/A_{Smin} calculated from M_{LL} of bridge with and without interval diaphragms. Please note that a continuity factor of *0.8* is introduced to account for the continuous slabs over three or more supported girders (AASHTO Standard, 2002) and the live load moment factor of *1.75* (*1.75**LL***) is not taken into consideration.

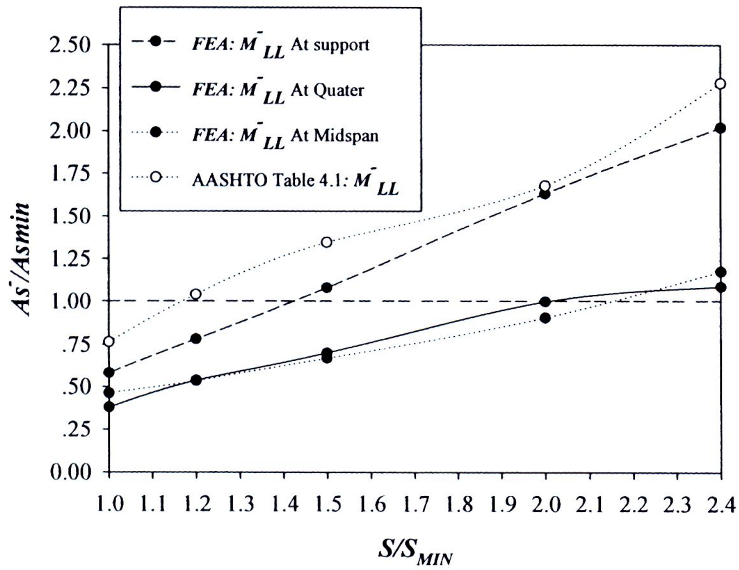

(a) Maximum M^-_{LL}

Figure 5.12 Reinforcement ratios A_S/A_{Smin} due to M_{LL} (with interval diaphragms): (a) Maximum M^-_{LL} ; (b) Maximum M^+_{LL}

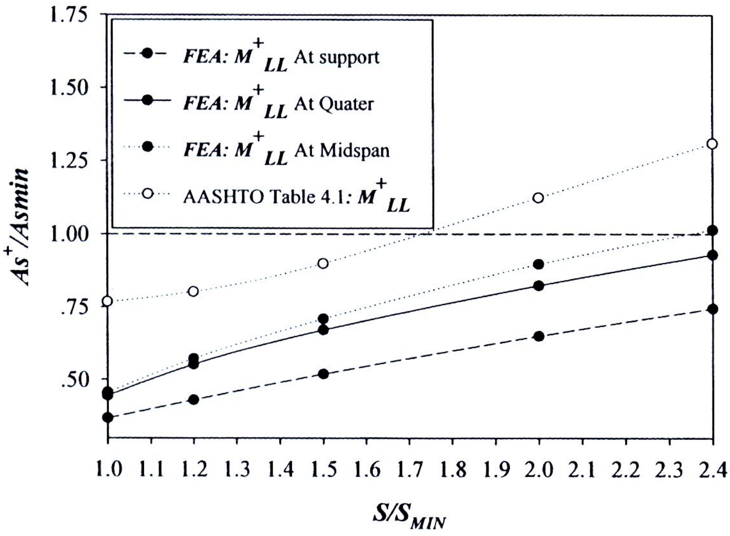

(b) Maximum M_{LL}^{+}

Figure 5.12 (Con't) Reinforcement ratios A_S/A_{Smin} due to M_{LL} (with interval diaphragms): (a) Maximum M_{LL}^{-}; (b) Maximum M_{LL}^{+}

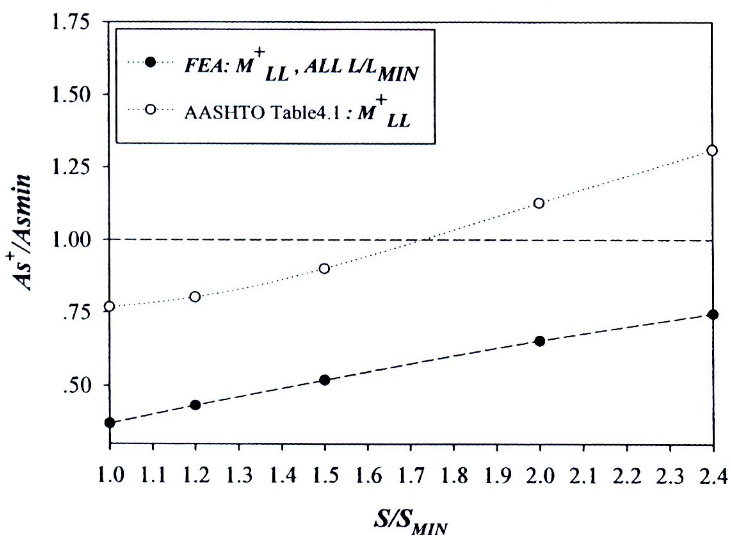

(a) At Support

Figure 5.13 Reinforcement ratios A_S/A_{Smin} due to Maximum M_{LL}^{+} (without interval diaphragms): (a) At support; (b) At quarter span; (c) At mid span

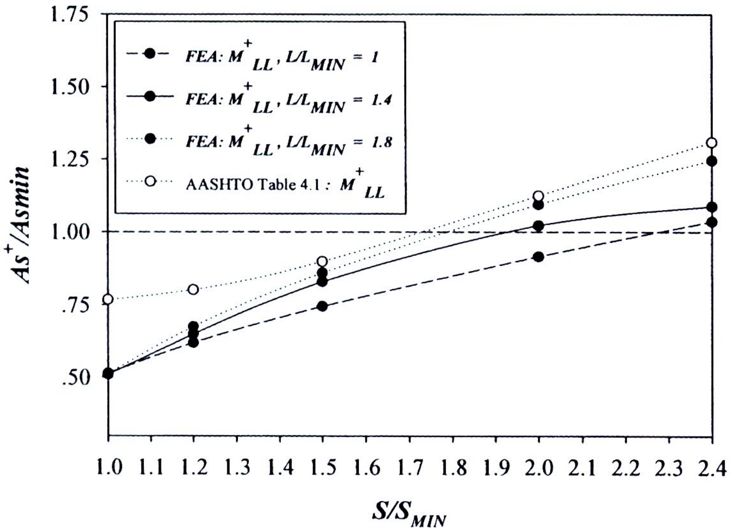

(b) At Quarter

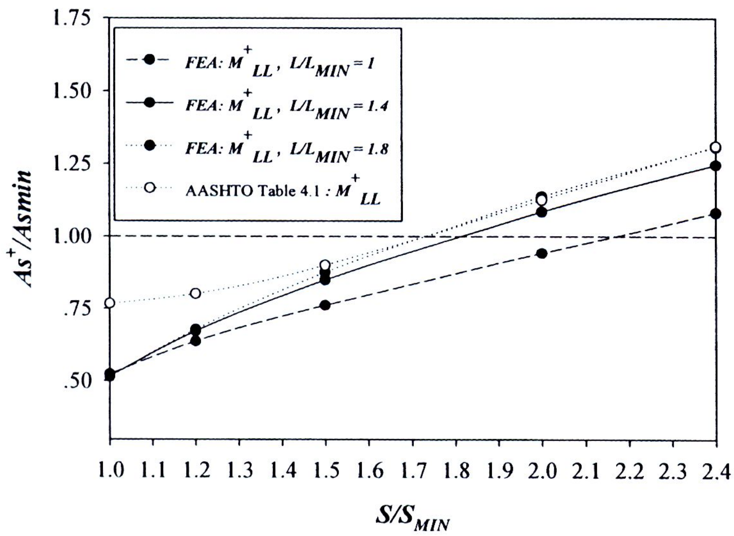

(c) At Midspan

Figure 5.13 (Con't) Reinforcement ratios A_S/A_{Smin} due to Maximum M^{+}_{LL} (without interval diaphragms): (a) At support; (b) At quarter span; (c) At mid span

Due to the advantage of the girder flexibility ($y \geq S$), which can result in a relatively low negative bending moment M^{-}_{LL} in a deck (especially when $S/S_{MIN} \leq 1.5$), much lower A_S calculated from the present study than the requirement of A_{Smin} can be noticed. This leads to the ratio of A_S/A_{Smin} less than unity as shown in Figure 5.12 (a). Therefore, the upper reinforcing bars may govern by A_{Smin} rather than A_S calculated from the live load moment M^{-}_{LL} in case of small S/S_{MIN}. However, the amount of upper reinforcing bars due to AASHTO Strip Method is mostly higher than A_{Smin} except in case of $S/S_{MIN} = 1$.

In relation to A_S due to M^+_{LL} (lower reinforcing bars), the girder flexibility ($y \geq S$) appears to affect M^+_{LL} when $S/S_{MIN} < 2$. It is noted that A_S due to the present FEA should governed by A_{Smin} when the bridge without interval diaphragms and $S/S_{MIN} < 2$ is considered as shown in Figure 5.13. The AASHTO Strip Method shows the same tendency for this topic.

Table 5.6 and Figure 5.14 show the ratio of reinforcement A_S/A_{Smin} due to dead load moment M_{DL}. The numerical results show very small values of A_S/A_{Smin} since the effect of this load type appears to be insignificant as discussed previously in section 5.7. It should be noted that A_S/A_{Smin} calculated from M^-_{DL} is more conservative than those due to M^+_{DL}. However, their magnitudes are rather small compared with M_{LL}.

Table 5.6 Ratio of reinforcement (at support) due to M_{DL} and M_{LL}

S/S_{MIN}	Ratio of reinforcement, A_S/A_{Smin} *			
	Negative ***M***		Positive ***M***	
	M^-_{DL}	M^-_{LL}	M^+_{DL}	M^+_{LL}
1	0.055	0.580	0.037	0.368
1.2	0.083	0.782	0.055	0.430
1.5	0.131	1.079	0.088	0.518
2	0.222	1.633	0.148	0.650
2.4	0.319	2.020	0.213	0.745

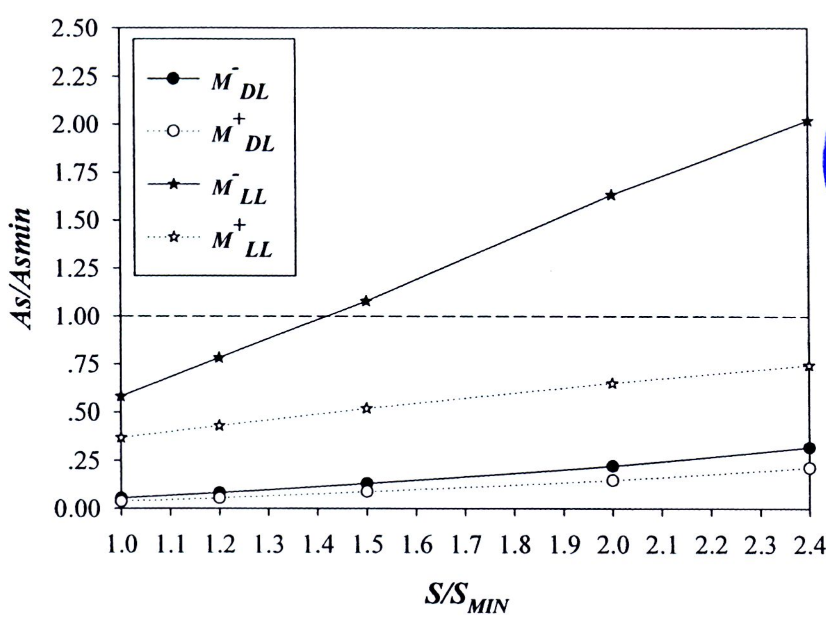

Figure 5.14 Reinforcement ratios A_S/A_{Smin} due to M_{LL} and M_{DL}